DIFFUSION OF CHEMICALS INTO GREEN WOOD

A Dissertation
Presented to
The Academic Faculty

by

Aaron Jacobson

In Partial Fulfillment
of the Requirements for the Degree
Paper Science and Engineering in the
School of Chemical and Biomolecular Engineering

Georgia Institute of Technology
May 2006

DIFFUSION OF CHEMICALS INTO GREEN WOOD

Approved by:

Dr. Sujit Banerjee, Advisor
School of Chemical and Biomolecular Engineering
Georgia Institute of Technology

Dr. William Koros
School of Chemical and Biomolecular Engineering
Georgia Institute of Technology

Dr. Tim Patterson
School of Mechanical Engineering
Georgia Institute of Technology

Dr. Yulin Deng
Chemical and Biomolecular Engineering
Georgia Institute of Technology

Dr. Lucian Lucia
Department of Wood and Paper Science
North Carolina State University

Date Approved: April 07, 2006

To my wife Kat, the greatest thing to happen to me.

ACKNOWLEDGEMENTS

First, I would like to thank my advisor, Dr. Sujit Banerjee for guiding me through my graduate studies. There were some difficult times during my years at Georgia Tech, but he helped me see the light at the end of the tunnel.

My wife Kat deserves credit for helping me through graduate school. She was very supportive of my quest to become Dr. Jacobson, and she helped me push through some difficult times.

I have a great set of parents who did a great job of raising me and emphasizing doing well in school and setting your goals high. Thanks, Mom and Dad. My sister Laura for ensuring that I was born, with countless wishes for a little brother. My sister Kathy for being a good role model while I was growing up. My sister Connie for helping me through undergraduate with numerous care packages and encouraging me to attend grad school. My twin sister Amy, for being excellent competition and for being a good friend when we weren't living at home together.

For my friends and colleagues at IPST and Georgia Tech, in particular, Dr. Tim Patterson for all the extra work we did together, Greg Fike for being a good mentor, and Cameron Thomson for countless academic debates.

TABLE OF CONTENTS

Page

LIST OF TABLES

Page

LIST OF FIGURES

Page

SUMMARY

Mass transport of chemicals into wood is important in kraft pulping. This thesis models small wood particles as cylinders and monitors how tritiated water and sulfide diffuse into the water-filled pores. Tritiated water diffusion is Fickian and diffuses completely into the water contained in the wood. Tortuosity values of the aspen and pine are tabulated. As particle size decreases, the tortuosity of the particles increases. As sulfide diffuses into wood, it is occluded from some water filled areas. Charge exclusion is a possible explanation for this. Sulfide and hydroxide transport into wood chips was displayed using indicators for each component. Pictures show sulfide ingress into the chip core faster, thus confirming the diffusion results. Fractionated sawdust was pulped to determine particle size effect on cooking and pulp properties.

CHAPTER 1

INTRODUCTION

Kraft pulping of wood has been practiced for over 100 years and has been extensively studied. The main focus of the research is on the chemical reactions of the reacting species hydroxide and sulfide with the wood constituents, lignin and cellulose. The delignification and cellulose degradation reactions do not occur in a homogenously mixed slurry. Lignin and cellulose are fixed components in wood and the chemical species must first enter and diffuse through the wood to react. In a chemical reaction, the availability of the reactants will influence the rate of the reaction. A chemical reaction will not proceed without reactants in place.

In kraft pulping, chemicals must diffuse through the water filled pores of wood to react with lignin and cellulose. In completely water-saturated wood, the only method of chemical transport is via diffusion. The purpose of this thesis is to study how chemicals diffuse into water saturated wood. The rate of diffusion of water into saturated wood is a reference point against which the uptake of other compounds can be benchmarked. The use of tritiated water (HTO) allows such a measurement to be made. Tritiated water is a conservative tracer for water; *i.e.* it moves with water and can be used to track water flow.

Treatment of wood with high sulfide solutions has been shown to increase the efficiency of kraft cooking. This thesis examines how sulfide diffuses into wood with respect to isotopic water and discusses some of the controlling factors.

The unique aspect of the thesis involves the use of a conservative tracer to examine how water diffuses into a water saturated material. The model development and diffusion analysis has not been for wood for this type of system. The results indicate that charge exclusion may occur with anions leading to different diffusion rates during kraft pulping of the two main cooking chemicals, sulfide and hydroxide.

CHAPTER 2

LITERATURE REVIEW

2.1 Diffusion

Diffusion is a transport phenomenon that describes the movement of matter or energy. It is typically stated that thermal or mass diffusion occurs when there is a temperature gradient or a concentration gradient. When those gradients exist there is certainly heat or mass transfer occurring via diffusion, but diffusion can occur even in the absence of heat or mass transfer. Diffusion is ultimately caused by the inherent energy of the atoms and molecules. Diffusion can occur without heat or mass transfer because the diffusion in each direction balances out.

2.1.1 History of Mass Transfer and Diffusion

Atoms and molecules exhibit random motion even though there is no external driving force for movement. This random motion is known as Brownian motion, and is credited to Robert Brown, a Scottish botanist who observed pollen grains suspended in water in quartz that exhibited a jittery motion. He also observed dust behaving in a similar fashion to rule out the motion was caused by some "life" process[1]. The origin of the motion was still undetermined.

In 1855, Adolph Fick, a German physiologist postulated the concept of diffusion by analogy to Fourier's law of heat conduction[2]. Thus, Equation 2.1, Fick's first law

$$J_x = -D\frac{\partial c}{\partial x} \tag{2.1}$$

was born. Here J_x is the diffusion flux in the x-direction, D is the diffusion coefficient, c is the concentration and x is the position. There was no explanation as to why diffusion coefficients were different for different molecules and no connection was traced to Brownian motion.

In 1905 Albert Einstein and Marian Smoluchowski provided an explanation of Brownian motion. They reasoned that if the kinetic theory was true, then water molecules would randomly move and collide with suspended particles, thus giving a random motion to the suspended particle[3]. The random collisions to the particles would explain the motion observed by Brown. The diffusion process could be mathematically described by a statistically driven spreading process using the random walk analysis. Random walk analysis in this case is based on the diffusing molecule taking successive steps each in a random direction

2.1.2 Diffusion of Gases

Diffusion of gases can be mathematically modeled easily due to molecular spacing; intermolecular forces can be neglected. In gas mixtures, the diffusion coefficient can be accurately predicted using kinetic theory.

For an ideal gas, kinetic theory can be applied, and the diffusion coefficient can be assumed to be proportional to the mean molecular velocity and the mean free path[4]. The mean free path and mean molecular velocity can be stated in terms of the empirically measured parameters pressure, temperature, and molecular weight and combined to give an equation to predict the diffusion coefficient. The semi-empirical Equation 2.2

$$D_{ab} = 4.3\times10^{-9} \frac{T^{3/2}}{P(V_A^{1/3} + V_B^{1/3})^2}\left(\frac{1}{M_A + M_B}\right)^{1/2} \tag{2.2}$$

was proposed by Gilliland, where

D_{ab} = diffusivity of a in b, m^2/s,

T = absolute temperature, K

M = molecular weight, kg/kmol

V = molar volume at the normal boiling point, m^3/kgmol

P = total pressure, atm

Gilliland's equation is adequate, but another equation proposed in 1966 is more accurate. Fuller et al. [5] derived Equation 2.3, which stems from curve fitting to experimental

$$D_{ab} = \frac{1.0\times10^{-9} T^{1.75}}{P[(\sum v)_A^{1/3} + (\sum v)_B^{1/3}]^2}\left(\frac{1}{M_A + M_B}\right)^{1/2} \tag{2.3}$$

data. The diffusion volume $\sum v$, is the sum of the atomic volumes for all the atoms in each molecule.

Another way to determine the diffusion coefficient for gases is to take into consideration the forces acting between molecules. The Lennard-Jones potential will describe the attractive and repulsive forces between atoms. Hirschfelder et al. [6] derived Equation 2.4 to predict diffusivity for nonpolar gases using the Lennard-Jones potential

$$D_{ab} = \frac{1.858\times10^{-27} T^{3/2}}{P\sigma_{AB}^2 \Omega_D} \left(\frac{1}{M_A + M_B}\right)^{1/2} \tag{2.4}$$

where σ_{AB} = collision diameter, m

Ω_D = collision integral

The collision diameter and collision integral are estimated using the Lennard-Jones potential, and will not be covered in this discussion.

2.1.3 Diffusion of Liquids

Liquids are more difficult to model than gases and solids. Liquids have strong intermolecular forces but are not ordered like atoms and molecules in a solid. Thus, describing the liquid state quantitatively is difficult. These difficulties have given rise to many experimental techniques to measure diffusion coefficients.

There are three approaches to predicting diffusivities in the liquid state. They are hydro-dynamical, quasi-crystalline, and fluctuation theories. Most equations are based on hydro-dynamical theory that relates diffusion to the viscosity or the difficulty of liquid

movement. The Stokes-Einstein equation gives the physical interpretation that a solute molecule represented by a hard sphere moves through solvent molecules that are much smaller. Stokes described the force acting on an atom and Einstein proposed Equation 2.5 relating the diffusion coefficient to the mobility of the atom

$$D = \frac{kT}{6\pi r\mu} \tag{2.5}$$

where k = Boltzmann's constant

r = particle radius

μ = viscosity

The model has many drawbacks that arise from its simplifications of molecular interaction, but it does predict diffusion coefficients within an order of magnitude[7].

Equation 2.6, an accurate modification of the Stokes-Einstein equation was introduced

$$D_{AB}^{\circ} = \frac{1.17\times10^{-13}\left(\xi_B M_B\right)^{1/2} T}{V_A^{0.6}\mu} \tag{2.6}$$

for predicting diffusivity in dilute solutions of nonelectrolytes[8].

Here μ = viscosity of solution (cP)

V_A = molar volume of solute at the normal boiling point (m^3/kgmol)

ξ_B = association factor of solvent B

The association factor ranges from 1.0 to 2.6 and accounts for interactions of the solvent. The factor is 1.0 for non-polar solvents, 1.5 for ethanol, and 2.6 for water. Equation 2.6, also called the Wilke-Chang equation usually gives results within ten percent of experimental data when water is the solvent. The error increases slightly when using organic solvents and is not suited for predicting diffusivity when water is the solute[9].

The Wilke-Chang equation does not hold for concentrated solutions. Diffusion for liquids is dependent on the concentration. Vignes proposed that since most concentrated solutions are non-ideal, then the non-ideality is responsible for changes in the diffusion coefficient[10]. Leffler and Cullinan expanded on Vignes equation to include the changes in viscosity at different concentrations[11] resulting in Equation 2.7.

$$D_{AB}\mu_m = \left(D^{\circ}_{AB}\mu_B\right)^{x_B}\left(D^{\circ}_{BA}\mu_A\right)^{x_A}\left(1+\frac{\partial \ln \gamma_A}{\partial \ln x_A}\right) \tag{2.7}$$

Here $D°_{AB}$ = diffusion coefficient independent of concentration

μ_m = viscosity of the mixture

x = mole fraction

γ_A = activity coefficient

If viscosity data are known for the mixtures and the individual components, the Leffler and Cullinan equation is accurate for predicting diffusion coefficients in concentrated solutions.

2.1.4 Diffusion in Solids

Diffusion in solids is much slower than diffusion in liquids and gases. In crystals, a diffusing molecule must displace a lattice molecule, transport into a void, or be able to migrate through the interstitial areas of the crystal lattice. Some of these diffusion mechanisms require high activation energies to proceed. In other solids, diffusion may occur via a diffusion path such as a grain boundary or a surface. When these diffusion paths are present, the diffusivity can be orders of magnitude higher than the diffusivity in the perfect solid. Depending on the mechanism, the diffusion coefficient in solids can range from 10^{-10} m^2/s to 10^{-37} m^2/s.

Diffusion in porous solids is a special case of diffusion and is very important for reaction in solids and catalysis. There are two primary types of diffusion in porous solids, ordinary and Knudsen diffusion. In ordinary diffusion, the mean free path of the diffusing molecule is much smaller than the pore diameter of the material. In cases where the diameter of the pore is smaller than the mean free path of the diffusing molecule, Knudsen diffusion will occur. There is also a transitional area where both bulk diffusion and Knudsen diffusion occur[12].

In Knudsen diffusion, the diffusing molecules contact the pore walls more often than they contact other molecules. The molecules adsorb to the surface of the pore and then desorb in a totally random direction. For straight round pores the Knudsen diffusion coefficient is calculated by Equation 2.8.

$$D_{K,a} = 97.0\, r \left(\frac{T}{M_a} \right)^{1/2} \tag{2.8}$$

Where $D_{K,a}$ = Knudsen diffusion coefficient (m^2/s)

r = pore radius (m)

Diffusion in porous solids occurs through void spaces in the material. Therefore, the porosity of the material is accounted for. In addition, the pores of a material are usually not perfectly straight. The tortuosity is a measure of how pathways wind and meander through the material. An effective diffusion coefficient can then be described as:

$$D_{a,e} = D_a \frac{\varepsilon}{\tau} \tag{2.9}$$

where $D_{a,e}$ = effective diffusion coefficient for a

ε = porosity of the solid

τ = tortuosity factor of the solid

The above equation can also be directly translated for calculating effective Knudsen diffusion coefficients. In cases where both Knudsen diffusion and bulk diffusion occur in a porous solid the effective diffusion coefficient for a species is calculated by:

$$\frac{1}{D_{a,e}} = \frac{1}{D_{a,K,e}} + \frac{1}{D_{a,B,e}} \tag{2.10}$$

In Knudsen diffusion pressure does not affect the diffusion coefficient. In porous solids, if the diffusion is influenced by pressure, it is an indication that the diffusion is influenced by the bulk diffusion coefficient.

2.2 Wood

2.2.1 Background

Trees have been utilized by ancient man for fuel and building structures, and in modern times are still used for those same purposes. In order to study the diffusion of materials into wood particles, the structure and composition of wood must be presented.

There are three directions when describing a tree, longitudinal, radial, and tangential. The longitudinal direction runs along the long axis of the tree. The radial direction runs from the center of the tree to the outside. The tangential direction curves around the tree.

Besides direction, there are three faces to the tree. First, there is the cross section view, which is exposed when the log is cut at right angles to the long axis. The tangential surface is the plane viewed if the bark was stripped off. Finally, the radial surface is viewed when the cut follows a radius of a tree along the long axis. These planes are illustrated in Figure 2-1.

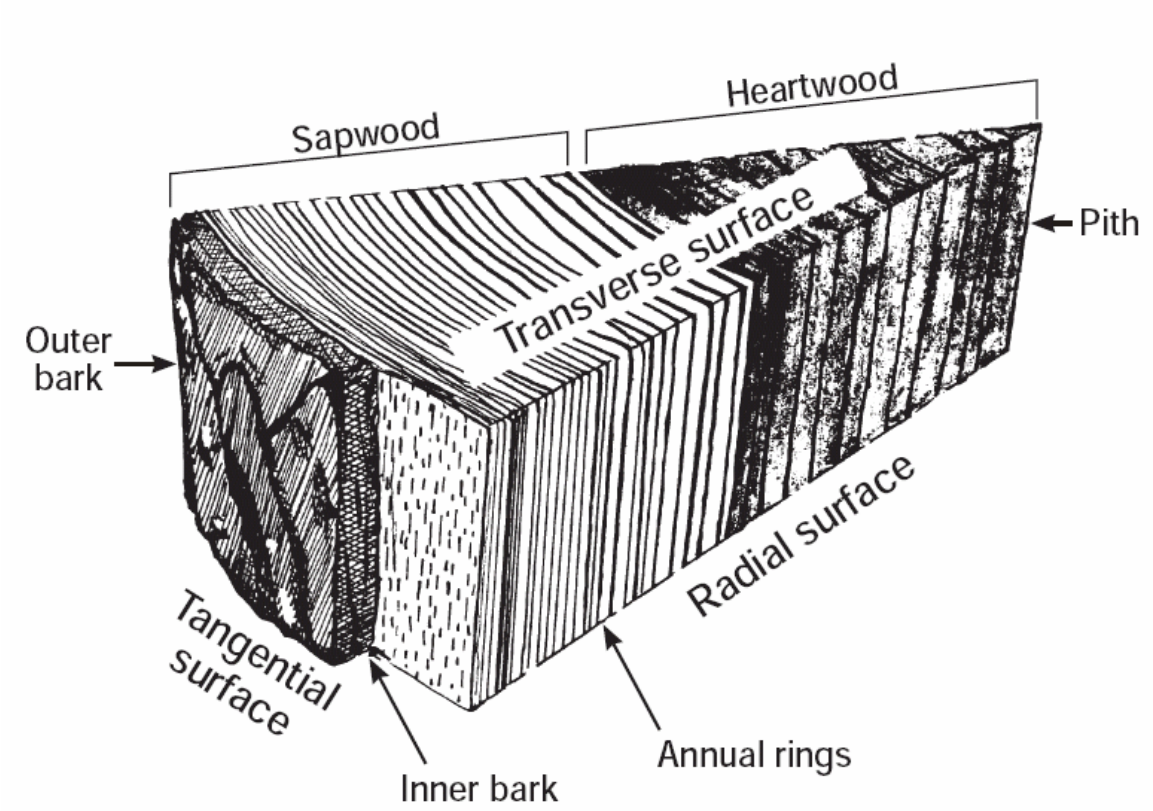

Figure 2-1 Section of a tree showing the planes of wood[13]

2.2.2 Tree Classification

Present day trees belong to the division spermatophytes in the evolutionary classification. There are two subdivisions of spermatophytes, angiosperms and gymnosperms. In the gymnosperm subdivision, which includes shrubs as well as trees, there is the coniferales class or conifers. Conifers can be classified as trees which have exposed seeds on the scales of cones. Conifers are also generally known as softwoods. Broadleaf trees are classified as angiosperms, commonly known as hardwoods. The angiosperm subdivision is split into dicotyledons and monocotyledons and includes grasses and herbaceous plants.

2.2.3 Structure of Coniferous Wood

Viewing the transverse of cross-section plane of a tree, light and dark areas form concentric rings. The light part of the ring is called earlywood or springwood and is formed during the beginning of growth in the spring. The darker region of the ring is the latewood or summerwood and is formed in the later part of the growth season. The transition between earlywood and latewood can be gradual or abrupt, allowing for differentiation between species of wood. The average composition of softwoods is shown in Table 2-1 [14].

Table 2-1 Composition of typical softwood

Component	% by weight
Cellulose	42 ± 2
Hemicellulose	27 ± 2
Lignin	28 ± 3
Extractives	3 ± 2

Close examination of a cross-section view of a tree shows a honey-comb type structure, with openings that differ in size. Closer examination shows a tubular structure with pointed ends. These structures are the tracheids or wood fibers. In addition to the fibers, there are structures that start from the center of the tree and point radially outwards towards the bark in a straight line. These are known as wood rays. Tracheids of softwood trees have a length of around 3 millimeters with a diameter of 30 micrometers[15]. Softwood tracheids are single cells while rays are composed of many small cells of about 0.25 millimeters in length. The volume proportion of rays in softwoods is small. In hardwoods, the tubular structures are simply called fibers.

Some conifers such as pine and Douglas fir contain resin ducts. Resin ducts are three times the diameter of a tracheid and are lined with small ducts that secrete resin. These ducts can run along the long axis of the tree and radially from the center. The radial canals are slightly small in diameter to the axial canals.

Fibers are connected to each other by the middle lamella. The middle lamella is comprised of mostly lignin and acts a glue or matrix to keep everything in place. There are also pits on the tracheids that allow material to be transferred between fibers. Figure 2-2 is a cross-section view of a softwood showing earlywood and latewood fibers.

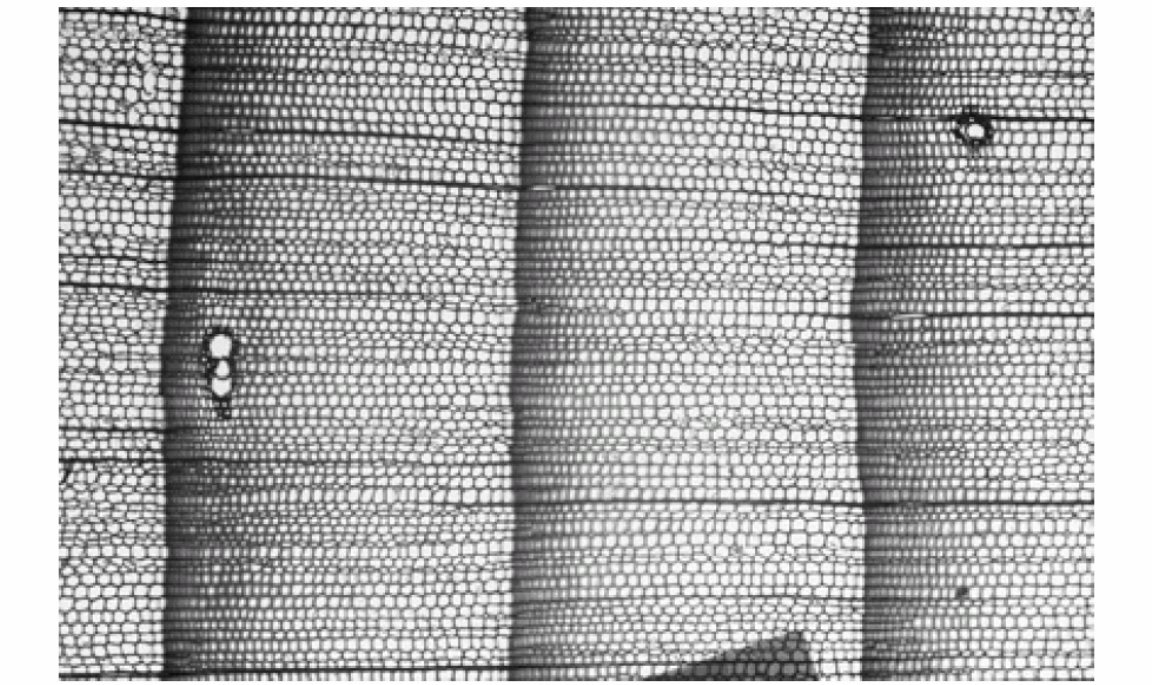

Figure 2-2 Cross-section view of softwood [13]

2.2.4 Structure of Hardwood

The most distinct characteristic of a hardwood that separates it from conifers is the presence of vessel elements. Vessel elements have larger cross-sections than fibers, and are used for the conduction of sap. The individual vessel elements are short, generally around 1 millimeter long, but are connected together to form longer structures. Some species of hardwood contain numerous vessel elements with large openings, giving a porous appearance. Hardwoods are classified by the arrangement of its vessel elements. Vessel elements that are uniformly distributed throughout the growth rings are diffuse-porous woods. Ring-porous hardwoods have rows of large pores next to each other in earlywood and smaller pores in latewood.

Rays of hardwoods are more developed and easily seen on transverse or tangential views. Hardwoods also form tyloses in the heartwood or center region of the tree. Tyloses are ingrowths that restrict the passage of material. Hardwoods also have shorter length fibers, around 1 millimeter long. Figure 2-3 is a picture of a hardwood showing fibers and vessel elements.

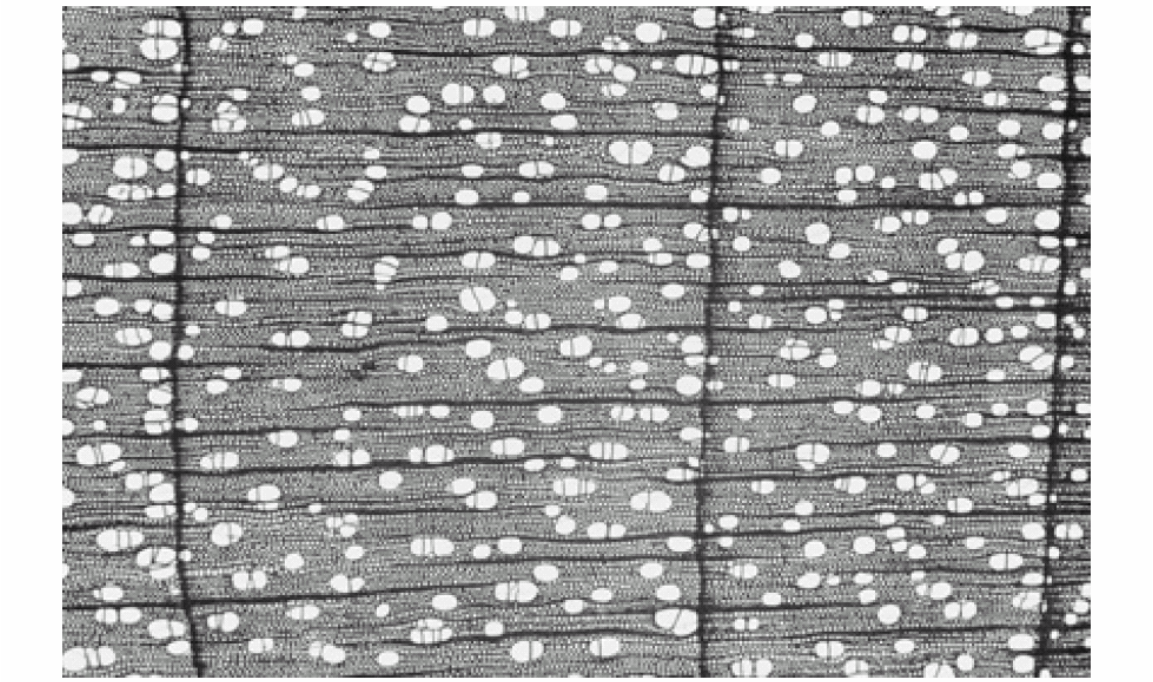

Figure 2-3 Cross-section view of hardwood [13]

2.2.5 Composition of a Fiber

The tracheids in a tree impart rigidity and strength and are valuable in papermaking. Tracheids have several parts, with each part varying in composition and size. Polymeric materials cellulose, hemicellulose, and lignin comprise the tracheid wall. There are also secondary components that may be in the tracheid such oils, tannins, and other extractives. However, these components do not impart any structural benefits to the tracheid. They do have an effect on color, odor, and biological resistance.

2.2.6 Cellulose

Cellulose is the main component of tracheids comprising 40 to 50 percent by mass. Cellulose is a polymer that is very resistant to chemical attack and is also difficult to

dissolve. Cellulose functions as the fibrous component that provides strength and has crystalline chains that are too closely packed for water to penetrate them. The repeating unit in cellulose is 1,4-β-linked glucose polysaccharide. Its structure is shown in Figure 2-4.

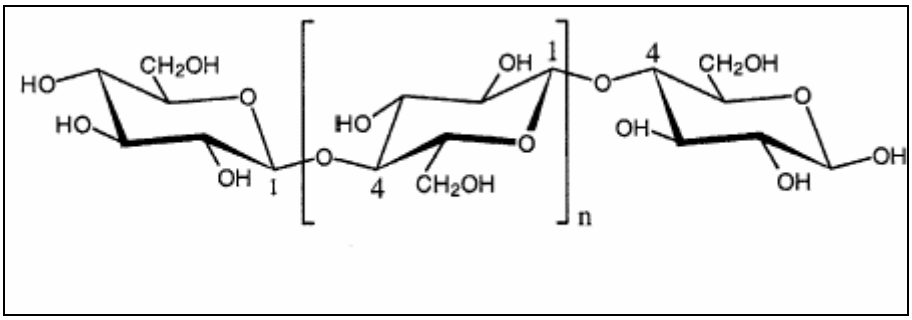

Figure 2-4 Chemical structure of cellulose – 1,4-β-linked glucose inside bracket [16]

Cellulose is insoluble in water and has a high degree of polymerization or number of repeat units in one macromolecule. In wood, the degree of polymerization is 10,000[17]. In cotton it is higher, reaching 15,000. The OH groups abundant on the cellulose chain result in lateral bonding to other cellulose chains. Cellulose chains may be in crystalline or amorphous forms.

2.2.7 Hemicellulose

Hemicelluloses comprise 20 to 35 percent mass of the cell wall and improve the structural properties of wood. These compounds provide bonding between cellulose fibrils via hydrogen bonding and through direct linkages. Hemicelluloses are made up of polysaccharides of different sugar monomers. Their degree of polymerization is much lower than cellulose, around 100 to 200 and may be linear or branched. Hemicelluloses

are completely amorphous. The principal hemicellulose in hardwoods is xylan, and the principal hemicellulose in softwoods is glucomannan. Hemicelluloses are soluble in dilute alkali.

2.2.8 Lignin

Lignin is an amorphous 3-dimensional polymer with the basic structural unit of phenylpropane. Lignin is a thermoplastic polymer, as it is heated above its glass transition temperature, it becomes rubbery. This corresponds to the onset of chain motion. As lignin is removed from wood, it loses its thermoplasticity. Lignin is insoluble and cannot be removed from wood without severe degradation due to its high molecular weight and 3-dimensional structure. Lignin is sometimes described as the "glue" that holds a tree together; a more accurate term is amorphous matrix that reinforces the tree.

Lignin is not hygroscopic in nature and provides a barrier to water penetration. Located in the cell wall, lignin acts as a bulking agent. It also reduces the dimensional changes that occur with moisture changes in the cell wall. The most important feature of lignin is the rigidity and stiffness it imparts to the cell wall.

Phenylpropane is a phenol ring that can be substituted with methoxyl groups. One methoxyl group addition gives the guaiacyl unit, while two additions give the syringyl unit. Softwoods contain guaiacyl lignin and hardwoods contain a copolymer of guaiacyl and syringyl lignin[18]. Figure 2-5 shows the structure of the building blocks of lignin.

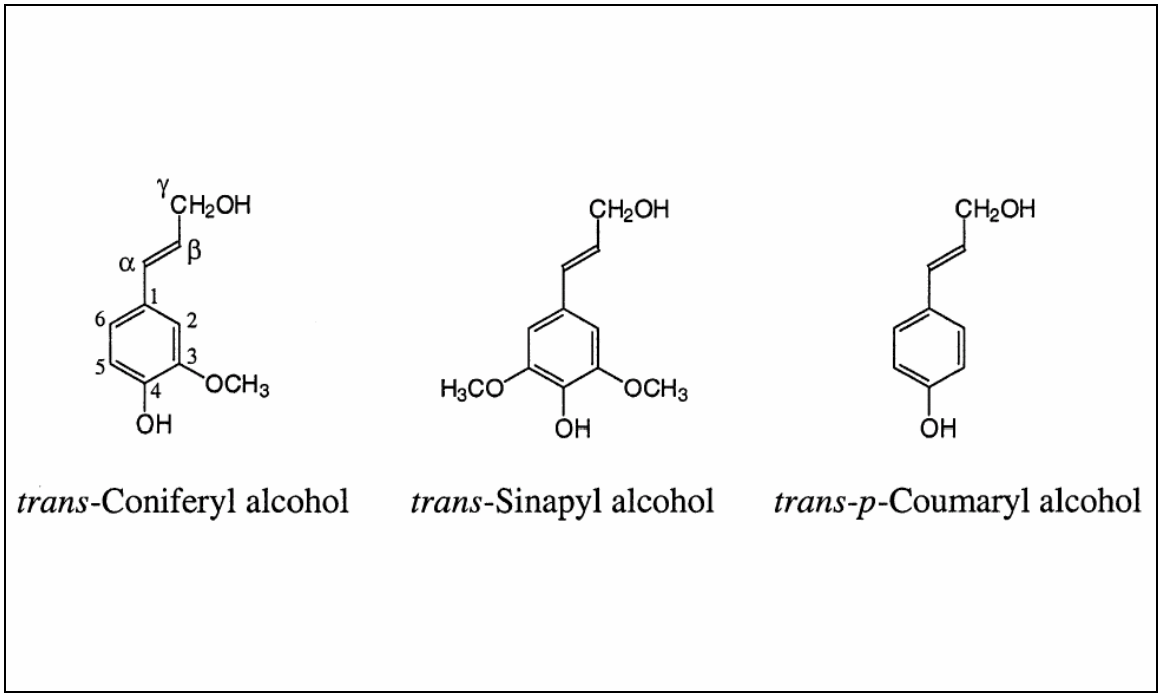

Figure 2-5 Building units of lignin [18]

The phenylpropane units are polymerized by the tree to form the complex form of lignin. Figure 2-6 shows a softwood lignin structure[19, 20].

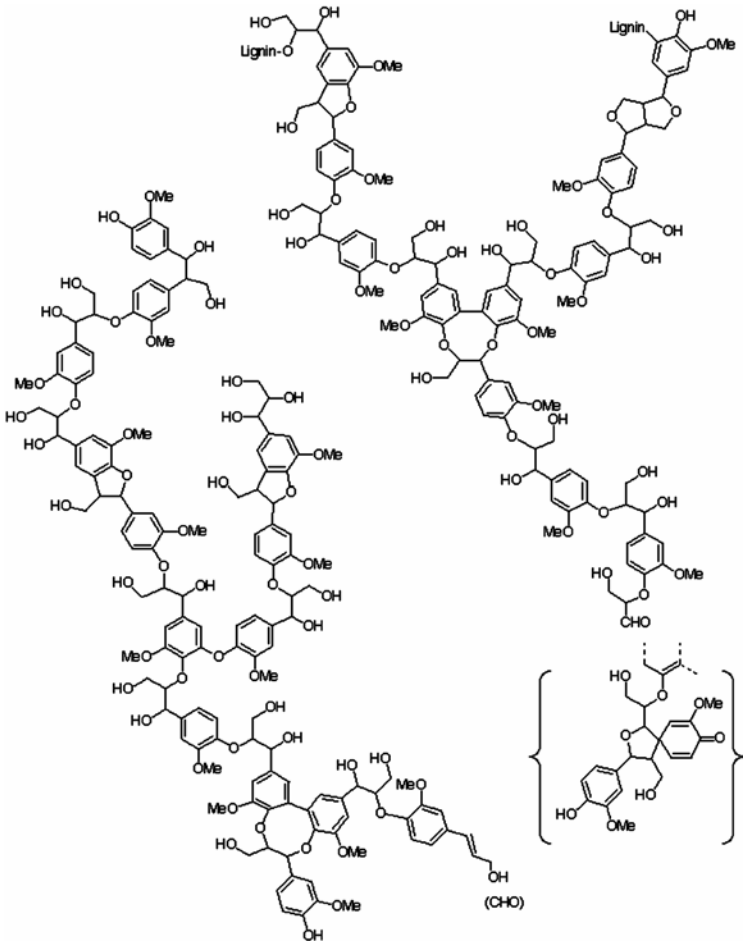

Figure 2-6 Softwood lignin [19]

2.2.9 Secondary Components

These fall into two categories, extractives and ash. The ash content of wood is low, typically less than one percent of oven dry weight for domestic trees. Calcium, potassium, and magnesium constitute the majority of the ash. These metals can be associated with the extractives or can be found in crystalline form.

Extractives encompass a wide range of organic compounds. They can be located in the cell wall or inside the cell lumen. Some extractives have economic importance; e.g. oleoresins, from which turpentine, tall oil, and rosin are distilled from wood.

Polyphenols are an abundant extractive and include tannins, anthocyanins, flavones, and lignans. The amount of extractives of wood is small, usually only a couple of percent of the ovendry weight of wood. Extractives do not impart any structural benefits to the wood but do have an effect on color, smell, and biological resistance.

2.2.10 Structure of Tracheid

The components mentioned in the previous section combine to form the cell walls or tracheids of the tree. The polysaccharides are ordered into clustered filaments also known as microfibrils. These long strands are 10 to 12 nanometers in width and 5 to 6 nanometers in thickness. Microfibrils contain long chains of cellulose encased in hemicellulose. Lignin surrounds and connects the microfibrils.

Microfibrils vary in orientation depending on location in the cell wall. As microfibrils are produced in the cell wall, lignin encases them and together forms a reinforced matrix. The microfibrils contribute high tensile strength along their axis while the surrounding lignin supplies plasticity. This combination gives wood its structural properties.

Microfibrils are not perfectly parallel and uniformly filled with lignin. There are void spaces present that allow for movement of moisture. These voids are long slender cavities called microcapillaries. The microcapillary volume is dependant on moisture content of the cell wall, with maximum void volume occurring with complete saturation of the cell wall.

The cell wall has several layers that vary in composition and microfibril angle. Figure 2-7 is a diagram featuring the various regions of the wood fiber.

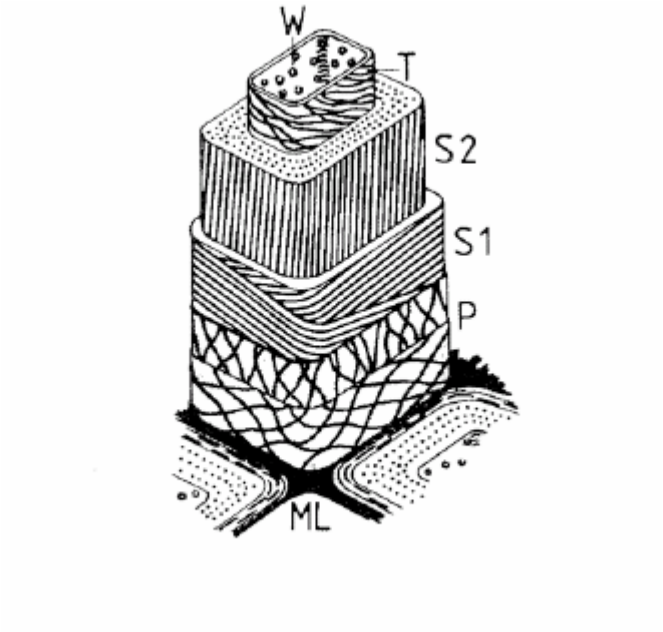

Figure 2-7 Cell wall layers of fiber showing primary fibril orientation [16]

The region between adjacent tracheids is the middle lamella. There are two parts of the middle lamella, the primary cell wall and the true middle lamella. The true middle lamella is almost all lignin and pectin. The primary wall is thin and contains mostly lignin and pectin. Since it is difficult to distinguish the separation of the two, they are combined and called the compound middle lamella.

The primary wall contains about 9 percent cellulose and is 0.1 microns thick in the living tree. Upon drying, the layer shrinks to 0.03 microns thick. The microfibrils in the primary layer are loosely interwoven. The microfibril angle in the primary wall is around 85 degrees with respect to the the cell axis.

The secondary cell wall is split into the regions S1, S2, and S3 layers. These are distinguished by layer thickness and microfibril orientation. The outside layer, S1 has microfibrillar groups that are in alternately crossed helixes. The S2 layer is much thicker and has microfibrils that are nearly parallel to the fiber axis. The S3 layer has microfibrils aligned perpendicular to the S2 layer. Each layer in the tracheid contains different amounts of lignin, hemicellulose, and cellulose. Figure 2-8 is a diagram showing the approximate percentages of materials in cell wall layers[21].

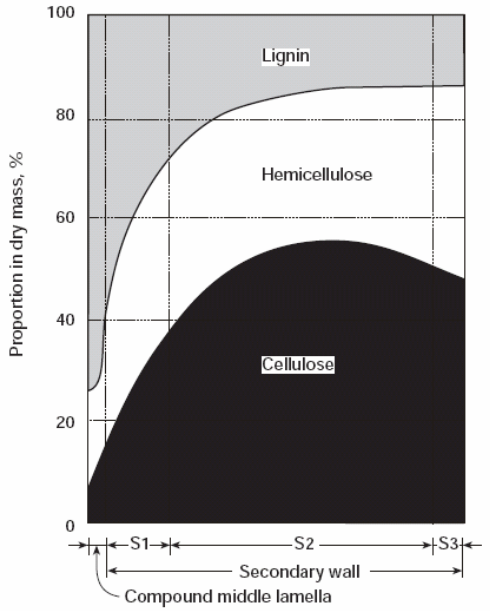

Figure 2-8 Percentage of components throughout cell wall [15]

The graph shows that the highest percentage of lignin is in the middle lamella. The S2 layer contains the most lignin by weight because it is such a large component of the tracheid.

A notable effect of the S2 layer having the majority of microfibrils oriented in the longitudinal axis is the hygroscopic dimensional changes. When wood gains moisture, water does not penetrate into the microfibrils, but goes between them. Since the S2 layer is the thickest, as wood gains moisture and swells, it swells in thickness. There is little or no dimensional change upon moisture changes in the axial direction of the fiber. This property of wood fibers has important ramifications in the production of paper.

2.2.11 Cell wall pitting

Cell walls have gaps or perforations in the secondary wall, creating a passage between adjacent fibers. These gaps or pits allow for material to be transported among the tracheids. Normally pits occur in pairs, located across each other on adjacent tracheids. Single or blind pits do occur when the other pit is missing or if it opens into the intercellular space. Figure 2-9 is a diagram of different kinds of pits.

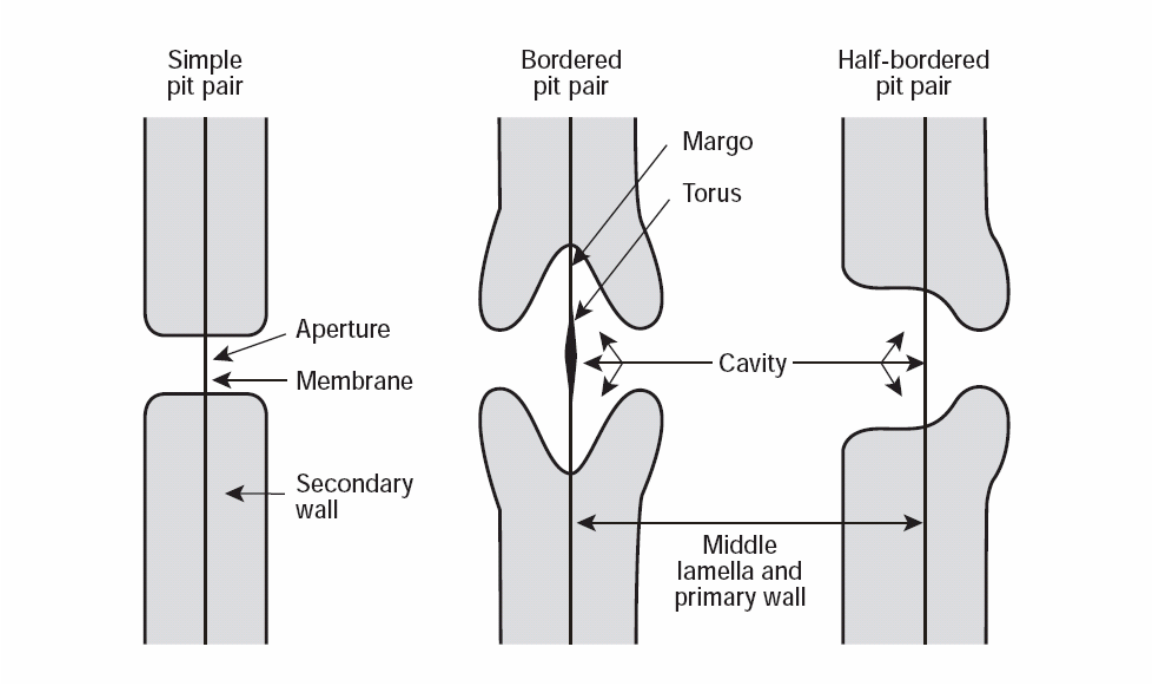

Figure 2-9 Types of pits and structures [16]

The pit cavity and the pit membrane are the primary parts of the pit structure. There are two types of pits, simple and bordered. Simple pits have uniform cavities while bordered pits have constricting cavities from the outside layer to the lumen. Pit pairs can be of similar or dissimilar pits. Most of the inter-tracheid bordered pits are along the tapered portions of the radial surfaces. The number of pits per softwood tracheid varies from 50 to 300 in earlywood; fewer in latewood[22].

Pits can become closed off or aspirated, thus restricting transport through them. Pits may also become closed due to extractive buildup or lignin encrustation.

Pit openings and cavities are quite variable, between latewood and earlywood, conifers and hardwoods, and between pits on the same tracheid. In softwoods, the pit may be

closed by a flat central plate called the torus. The torus is connected to the pit through radially oriented strands. The strands and the torus are located in the region of the pit membrane called the margo.

Tension wood forms in trees to stabilize the tree and branches. In softwoods, compression wood forms on the underside of leaning trees and branches. Virtually every tree has some compression wood, but the amount varies considerably from tree to tree. Compression wood is characterized by high density, rounded thick-walled tracheids, large fibril angles, highly lignified secondary wall, shorter fiber length, and spiral checks in the cell wall. The cellulose content of compression wood is only 30%, compared to 42% in normal softwood[23]. The lignin content can be as high as 40%. The lignin in compression wood is more highly condensed than a normal softwood lignin. Compression wood will cause problems in pulp manufacturing. Compression wood fibers do not respond well to refining.

2.3 Water and Wood

Water is essential to the tree for growth and sustenance. Water is taken up by the root system and transported throughout the tree. Once the tree is cut down, water uptake stops. The moisture content in the wood at this point is the green moisture content. The green moisture content is different between species of trees and can change depending on climate or location within the tree. While water is important to the living tree, it is a costly nuisance for wood-related industries. The amount of energy released by combustion of wood is inversely proportional to the moisture content. The higher the

moisture content, the more water is being shipped unnecessarily. However, removal of this water prior to shipping or burning can be quite costly and time-consuming.

The moisture content of wood is usually given as a percent, and is based on the weight of water per weight of dry wood. The moisture content is calculated by

$$M.C.\% = \frac{W_w}{W_o} \times 100 \tag{2.11}$$

where W_w is the weight of water in the wood and W_o is the ovendry weight of the wood. The weight of water is found by subtracting the ovendry weight of the wood from the wet weight of the wood.

2.3.1 Water in Wood

When wood cells are newly formed in a tree, they are saturated with water. Water is found in the cell wall and in the cell cavity or lumen. The wood cells stay saturated until they are no longer used for water conduction. As the liquid water leaves the lumen, it is replaced by water vapor. The water in the cell wall remains. In total, water in green wood is in three forms, liquid water in the lumen, water vapor in the lumen, and water in the cell wall. The liquid water in wood is classified again into bound and free water.

2.3.2 Bound water

Bound water is referred to the water that is found in the cell wall. The water is called "bound" because it is held strongly in the cell wall compared with normal liquid water. Hydrogen bonding between the water and the cell wall material are the cause of this increased interaction. As dry wood takes on moisture, bound water in the cell wall appears first until it is completely saturated. When the hydrogen bonds form between water and the cell wall, energy is released. This is the heat of wetting for dry wood. To remove this water, more energy must be supplied to break the hydrogen bonds. Due to the strong affinity by the cell wall for water, it is difficult to keep moisture out of the cell wall. This is why wood is defined as hygroscopic material. Bound water or hygroscopic water is found in the cell wall and is bound to the hydroxyl groups of neighboring molecules. Water primarily associates with the hydroxyl sites of the cellulose and hemicelluloses. The bound water moisture content is limited by the number of sorption sites available and by the number of molecules that can be held on a sorption site[24]. The crystalline regions of cellulose do not allow for water to enter. Their sorption sites are not accessible because adjacent cellulose molecules are bound to the sites. Fiber saturation point (FSP) is defined as the moisture content at which the cell walls are saturated with bound water with no free water in the lumens[25]. The bound water moisture content is dependant on the relative humidity and temperature of the surrounding air. The fiber saturation point varies depending on species but most species have a FSP of 30%.

Bound water is split into two categories: non-freezing bound water and freezing bound water. This phenomenon is observed in other polymeric materials containing hydrophilic regions. Differential scanning calorimetry (DSC) is a good tool to determine if materials containing water have freezing and non-freezing bound water and has been successfully used on fibers[26, 27] and wood[28]. Non-freezing water refers to water that is very tightly bound to the polar groups inside the cell wall. The interaction is strong enough that the water will not freeze even at temperatures below zero degrees Celsius. Freezing bound water is also associated with the cell wall but the interaction is not as strong. Freezing bound water has a melting point of less than zero degrees Celsius. The ice structures that do form are different from that which is formed in the free water regions of the wood fiber.

Although non-freezing bound water is associated strongly with the constituents in the cell wall, it is not immobile. Freezing bound water is likely several molecules away from the polar group. The first molecule around a polar group will be the strongly hydrogen bonded non-freezing water. It is likely that there is a group or layer of molecules near the polar unit that is non-freezing. Located a few layers past the non-freezing water is the less associated freezing water. There are two major schools of thought regarding the structure of water adsorbed onto the surface of wood. The water molecules either form layers upon the cellulose or they associate into water clusters[29]. In the cluster theory, water molecules form larger clusters in the bulk fluid, usually six water molecules per cluster[30]. When the clusters come near the surface of cellulose, the structures become smaller and then dimers and trimers of water are associated with the hydroxyl groups on

the cell wall[31]. In the layering theory, the water molecules near the surface are structured according to the cellulose[32]. Successive layers are formed on top of the previous layer. The attraction between layers decrease with distance from the surface based on Polanyi's theory of multilayer adsorption[33]. Movement of water during adsorption and drying is affected by the different types of water in the wood.

When only bound water is present in wood, the moisture content is related to the relative humidity of the air. As the humidity in the air changes, so does the moisture content of the wood. At a specific relative humidity the wood may have more than one value for moisture content. This is due to the fact that the moisture content of wood at a certain relative humidity is also dependant on whether the wood is adsorbing or desorbing water. Figure 2-10 shows this effect on cotton fibers[34]. This is called hysteresis and occurs in paper as well as wood.

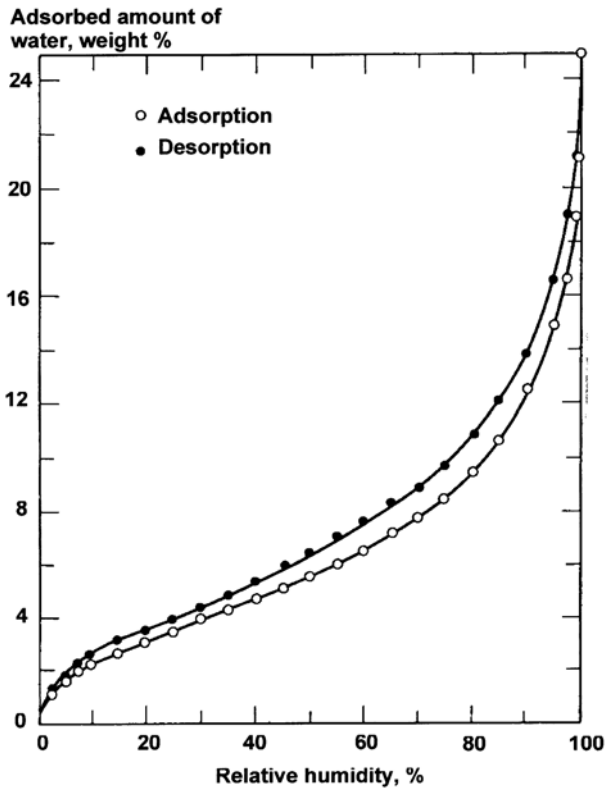

Figure 2-10 Hysteresis of Cotton Fibers [34]

As the bound water content changes so does the structural stability of wood. Bound water causes cell walls to expand and is responsible for the swelling of wood. Once the fiber saturation point has been reached, additional water will not cause dimensional changes. As water molecules transport into wood and become bound water, they associate to the hydroxyl groups of the cellulose and hemi-cellulose. In the cell wall, the majority of cellulose microfibrils are oriented in the longitudinal direction. Water that is adsorbed into these layers must fit in between the layers. As more water molecules adsorb in these areas, the water will force the layers apart, thus causing the swelling of wood. Figure 2-11 is a picture showing how a cotton fiber's dimensions change as relative humidity changes[35]. It is clear that dimensional changes due to swelling

primarily manifest themselves in the radial and tangential directions. The length is not significantly affected.

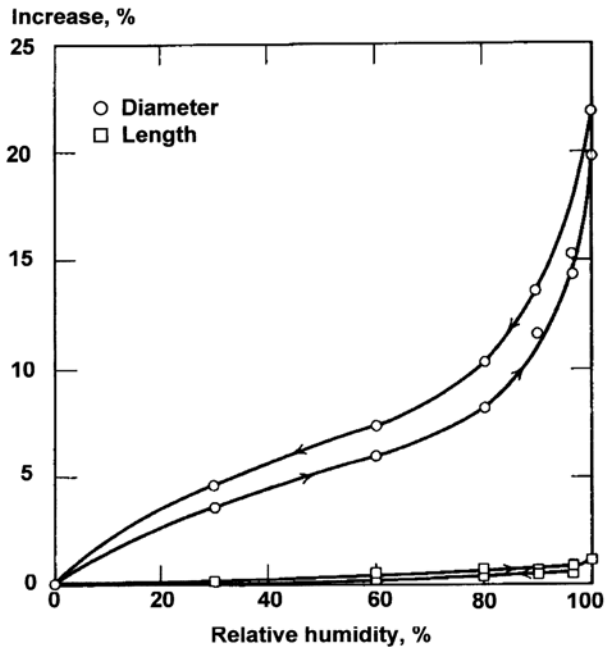

Figure 2-11 Dimensional stability of cotton fiber with changes in relative humidity [35]

2.3.3 Free Water

Free water is held in the lumen and has the same properties of bulk water. While dry wood is adsorbing water, the free water is the last to accumulate and the first to leave during drying. Movement of free water occurs through the pits between fibers. Water in the lumen is in equilibrium with the water in the cell wall. The amount of free water wood may hold is limited by the void space or porosity of the wood. Free water is not involved in hydrogen bonding to sorption sites. Free water is held only be weak capillary forces and cannot cause shrinking or swelling since the cell wall is all ready saturated with more tightly bounded hygroscopic water.

2.4 Kraft pulping

The first patents on Kraft pulping were granted to Eaton in 1870 and 1871 for the delignification of wood with a mixture of sodium hydroxide and sodium sulfide[36]. The origin of this technology was supposedly established sixty years earlier in England. Kraft pulping received its name from the Swedish language. In Scandinavia, sulfate (kraft) pulping was used to produce paper with high strength characteristics. Kraft is the Swedish word for strength.

Kraft pulping uses sodium hydroxide and sodium sulfide at a pH above 12. The wood chips are cooked at 160-180 degrees Celsius with a steam pressure about 800 kilopascals for one-half to three hours. The kraft process can pulp any wood species and gives high-strength pulp. The pulp is of lower yield and is more difficult to bleach than sulfite pulps. There is also a problem with the distinct odor of sulfur in its reduced form. The important variables of kraft pulping are:

- Wood species
- Chip geometry
- Ratio of effective alkali to wood weight
- Concentration of effective alkali
- Liquor to wood ratio
- Sulfidity
- H-factor (function of time and temperature)

Chip geometry and especially chip thickness is of great importance. Under cooked and over cooked pulp is a result of high variability in chip dimensions. The penetration for liquors at pH above 13 is almost the same in all three directions[37]. Complete penetration of the cooking liquor in to the wood chips is important for uniform pulping. The H-factor is a pulping variable that takes into account cooking and time and temperature and thus indicates extent of reaction.

There are three phases of delignification. Even at low temperatures, about 25 percent of the lignin can be removed relatively fast. This type of lignin is referred to as extracted lignin. The next phase is bulk delignification and will only proceed at temperatures above 150 degrees Celsius. The final phase, residual delignification, takes place much slower than bulk delignification.

2.4.1 Impregnation of wood

Uniform distribution of chemicals inside wood chips during pulping is essential for uniform delignification. Non-uniformity in impregnation leads to unfiberized wood (rejects), discolored pulp, lower final pulp yield, impaired bleachability, and detrimental effects on paper properties[38]. Chemicals and energy are transferred to wood chips in two phases. In the first phase, the penetration phase, chips are saturated with liquid containing chemicals before delignification occurs. In the second phase, chemical movement to reaction sites is controlled by diffusion.

Prior to the impregnation phase, the wood chips must be treated to remove the air inside. This is accomplished by steaming. Chips are treated with steam and the temperature inside increases and the air starts to expand. About 25% of the air is removed in this stage. The water in the chip will also be heated, thus increasing the vapor pressure of the water and driving out more air. Diffusion of steam inward will further reduce the air content of the chip. The steam will diffuse into capillaries of chips, condense, evaporate again, and displace air from the chips. The important variables in steaming are temperature, time and steam pressure. In the early 1900's, brief steaming of chips was done to facilitate uniform packing of the chips inside the digester[39]. The importance of air removal and the positive effects of steaming on penetration were discovered later.

2.4.2 Penetration

The steamed chips are then penetrated with liquor at an elevated pressure. The steam inside the chip condenses, which increases the pressure gradient between the free liquor and the interior of the chip. The rate of penetration depends on steaming conditions and applied pressure. Efficient penetration of cooking chemicals is important in pulping, and has been shown to increase pulping uniformity and reduce cooking time.[40, 41]

Penetration is the liquid transfer into the steam filled cavities of the chips. Two mechanisms drive penetration, capillary forces and pressure. Penetration by capillary forces is governed by Equation 2.12

$$h = \sqrt{\frac{r\,\tau\,t\,\eta}{2}} \tag{2.12}$$

where h - penetration distance

r – capillary radius

τ - liquid surface tension

t – time

η - liquid viscosity

Forced penetration by pressure is defined by Equation 2.13.

$$\frac{V}{t} = k\frac{n r^4 \Delta p}{L\eta} \tag{2.13}$$

where V – liquid amount entering capillaries

n – number of capillaries

Δp – pressure gradient

L – length of capillaries

k– material constant

In Equation 2.12, the capillary radius is raised to the fourth power and therefore has great impact on penetration. Dense wood has smaller capillary radii. Sapwood is penetrated faster than heartwood and early wood is penetrated faster than latewood. Wood pore structure is also important in penetration. Some hardwoods, although denser, will penetrate faster due to their more open pore structure. Raising temperature will also

increase penetration by reducing viscosity. However, an increase in liquor temperature will also cause the gases inside the wood to expand, and the solubility of air in the liquor will decrease[42]. This penetration takes place primarily in the longitudinal or fiber direction[43], hence chip length is important for complete liquid penetration. Reducing chip length has been shown to increase penetration[44]. However, chip thickness also plays a role in liquid penetration.

As chemicals penetrate and flow into the wood, the air trapped inside the chip starts to compress. Once the pressure inside the chips reaches the applied liquid pressure, the cooking chemicals no longer flow readily into the chip. The penetration of the chip enters a secondary phase. The ingress of liquid into the chip is now controlled by the dissolution of the air into the liquid and the subsequent diffusion of the dissolved air out of the chip. Chip thickness is important in this stage, as a thin chip has a smaller diffusion path length than a thicker chip[45]. Secondary penetration becomes important when the initial moisture content of the chip is low; for instance heartwood usually has a lower moisture content than sapwood. Liquid penetration under pressure usually takes place in a few minutes[46]. Then if saturation is not complete, secondary penetration starts, and can take much longer[47].

2.4.3 Diffusion

Once the penetration stage of impregnation is complete, the only way for chemicals to transport is via diffusion. Chemicals are consumed inside the chip, thus setting up a concentration gradient. Fresh chemicals diffuse into chip from the liquor surrounding the

chips while lignin and cellulose fragments diffuse out. Diffusion is the process by which matter moves from one part of a system to another as a result of random molecular motions. If the diffusion distance is too long or rate of diffusion too slow, the cooking chemicals are consumed before they reach the center of the chips. In diffusion, there is a critical balance between rate of ion transport, chip thickness, and rate of chemical reaction. Chemical reagents can only completely diffuse into chips that are fully penetrated. In fully penetrated chips, diffusion proceeds according to Fick's law, equation 2.14,

$$J_z = -D\frac{dc}{dz} \tag{2.14}$$

where J_z – rate of movement of material per unit area perpendicular to z direction

D – diffusion constant of diffusivity

dc/dz – concentration gradient in x-direction

The effective capillary cross sectional area (ECCSA) varies in uncooked wood according to grain direction. The porous structure is more open in the longitudinal direction than in the transverse or tangential direction. Figure 2-12 shows the ECCSA for partially delignified wood blocks at a pH of 13.2[48].

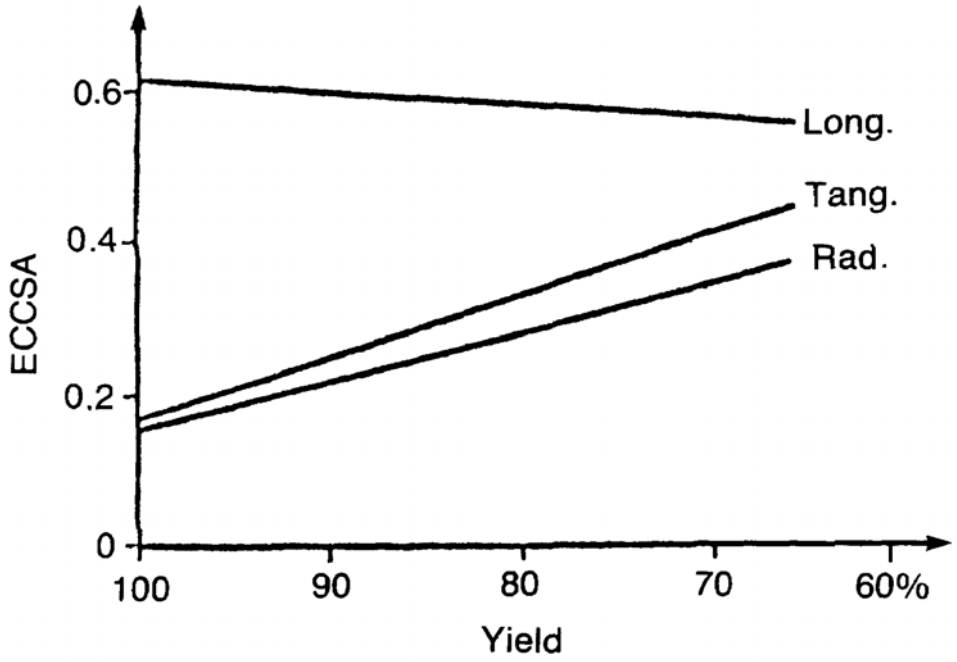

Figure 2-12 ECCSA of Wood at high pH [48]

The porosity of the cell wall increases as delignification proceeds, minimizing the difference in ECCSA for the three directions.

Temperature also has an effect on diffusion. Equation 2.15 describes the relationship between temperature and diffusivity

$$D = kT^{0.5}e^{\frac{-E}{RT}} \tag{2.15}$$

where k – frequency constant

E – activation energy

R – general gas constant

Increasing temperature will increase diffusion. The reaction rate of delignification is also temperature dependent. Equation 2.16 describes the reaction rate temperature dependence following Arrhenius law.

$$K = A e^{\frac{-E_a}{RT}} \tag{2.16}$$

Where K is the reaction rate if mass and heat transfer limitations are neglected. Comparing these two equations shows that reaction rates are more temperature dependent than diffusion rates. Figure 2-13 shows how the relative reaction and diffusion rate changes with temperature.

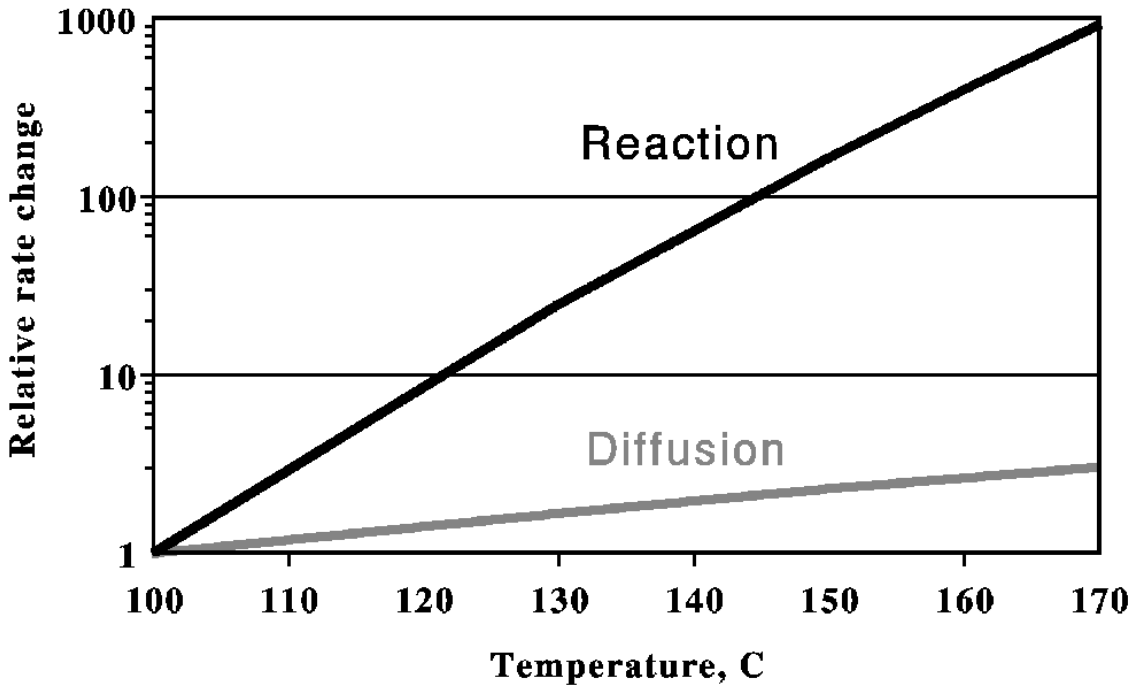

Figure 2-13 Reaction and Diffusion Rate Change vs. Temperature [49]

This means that non-uniform delignification develops in situations where diffusion rate is the controlling factor[49]. These situations may occur when impregnation is poor, impregnation liquor reagent concentrations are too low, or chips are very thick. Cooking chemicals are consumed too fast in the outer sections of the chips as they travel inward. Thus, the inner sections of the chips will be less delignified.

A correct chip size is vital for efficient pulping since path length is so important in chemical transport via diffusion. When chips are too large, the chemicals can not diffuse into the center regions of the chip as well as the outside. This causes an increase in the number of rejects. To keep the same number of reject levels with increasing chip size, the pulping temperature must be lowered[50]. This in turn also makes the cook last

longer which is never desirable. However, if there is inadequate diffusion and liberation of the fibers in batch digesters problems additional to a high rejects level can occur. For instance, the lignin content of the liberated fibers can be highly variable and it may be more difficult to empty or "blow" the digester.

2.4.4 Penetration and Diffusion Aids

There has been extensive work done on improving the impregnation process. They either deal with the chips themselves or the liquid penetrating the wood. They are usually classified in to four groups: air removal, surfactants, mechanical de-structuring of chips, and bio-treatment of chips. Mechanical destructuring of chips involves mechanical impact upon the chips to create fissures or cracks within the chip. The increase in fissures should allow more pathways for penetration.

As mentioned earlier, air removal is vital in liquor penetration of wood. In practice, this is done by steaming wood chips. This is a cheap and practical way to remove air from wood. Improvements in steaming of chips include improving the contact of steam with all the chips in the steaming vessel. There are other methods of air removal that have been investigated but are not practical. Vacuum treatment of dry chips was shown to be effective in air removal[43]. However, industrial cooking would not dry chips as it would require massive amounts of energy. With a low enough pressure it is possible to evacuate all the air by having the water boil at the low pressure and force the air out. Problems arise in chips due to extractives blocking passages and with surface tension forces in small capillaries that would counteract the pressure[51].

Bio-treatment of chips involves using enzymes or fungi or other biologically active substances that will react with wood. Pectinase and cellulase have been found to attack the pit membranes in softwoods and hardwoods and causing membrane dissolution[52, 53]. If all pit membranes in a chip were dissolved, this would greatly increase the penetration of chemicals. However, enzyme transport into the wood chip can be quite slow due to enzyme's large molecular size. The research that has been conducted with fungi is limited, but some have shown that some species of fungi will degrade extractives and or pit membranes[54].

2.4.5 Lignin reaction kinetics

Lignin comprises 70% - 80% of the middle lamella. This layer is thin compared to the secondary cell wall. The lignin content of the secondary cell wall is 20%, but due to its size, the secondary cell wall contains 70% - 80% of the total lignin. Wood chips maintain their shape even at 80% delignification. Thus it is likely that the lignin in the secondary wall will dissolve before the middle lamella lignin. Another reason for a slower delignification of middle lamella lignin is the relative higher amount of guiacyl nuclei.

During initial delignification, only lignin fragments that are small enough to dissolve will be extracted from the secondary cell wall. Equation 2.17 is the initial delignification equation

$$\frac{dL}{dt} = k_{il} e^{(17.5 - \frac{8760}{T})} L \qquad (2.17)$$

where L – lignin content at time t

k_{il} – a species specific constant

There is no hydroxide term in the initial delignification equation. This does not mean the reaction can proceed without hydroxide. The hydroxide concentration does not affect the rate of the reaction.

Once the temperature of cooking reaches 140°C, bulk delignification begins. Seventy to eighty percent of lignin is dissolved in this phase. Lignin breakdown starts in the cell wall and progresses to the middle lamella. Equation 2.18, the bulk delignification equation, is more complicated.

$$\frac{dL}{dt} = k_{0bl} e^{(35.5 - \frac{17200}{T})} [OH^-] L + k_{1bl} e^{(29.4 - \frac{14400}{T})} [OH^-]^{0.5} [HS^-]^{0.4} L \qquad (2.18)$$

Where $[OH^-]$ – hydroxyl ion concentration

$[HS^-]$ – hydrosulfide ion concentration

k_{0bl} and k_{1bl} – species specific constants

The relative reaction rate and activation energy are higher for the bulk delignification stage. The reaction is strongly dependent on hydroxyl and hydrosulfide ion

concentration. The reaction slows down as the concentration of dissolved lignin increases. The rate slows down in thicker chips as the rate is diffusion controlled.

The bulk delignification stage proceeds until about 90% of the total lignin is dissolved. The residual delignification stage then begins, and is considerably slower than the bulk delignification phase. Equation 2.19 is the residual delignification equation.

$$\frac{dL}{dt} = k_{rl} e^{(19.64 - \frac{10804}{T})} [OH^-]^{0.7} L \qquad (2.19)$$

Where k_{rl} – a species specific constant for residual delignification.

The hydroxyl ion concentrations effect on rate is less in this stage but its importance is not. If the alkali concentration is too low, dissolved lignin fragments will condense. Condensation of lignin is very undesirable and leads to reduced yield and pulp quality. Figure 2-14 shows delignification in the three stages.

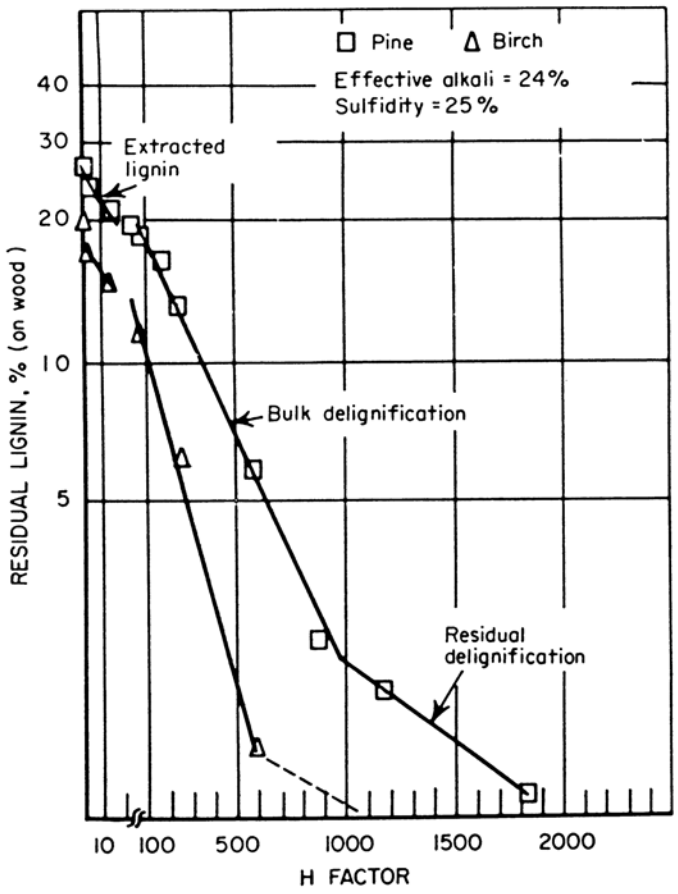

Figure 2-14 Lignin dissolution vs H-factor for two species of tree [49]

2.4.6 Carbohydrate reactions

Kraft pulping is not specific to lignin, carbohydrates also dissolve during a kraft cook. Most of the carbohydrates that dissolve do so during the initial delignification phase. Hemicelluloses dissolve more readily than cellulose in alkaline conditions.

During initial delignification, 75% of all carbohydrates that dissolve are glucomannans. Xylan dissolves at temperatures above 140°C but slows down during bulk delignification. Degradation of hemicelluloses leads to acid groups that consume alkali. Most of the

alkali is consumed during the initial and early bulk delignification phases to neutralize the acidic compounds. The dissolution rate of carbohydrates is related to delignification rate in all three stages. Equation 2.20 is the carbohydrate rate expression during initial delignification.

$$\frac{dC}{dt} = k_{ic}[OH^-]^{0.11}\frac{dL}{dt} \tag{2.20}$$

Equation 2.21 is the carbohydrate rate expression during bulk delignification.

$$\frac{dC}{dt} = k_{bc}\frac{dL}{dt} \tag{2.21}$$

Equation 2.22 describes carbohydrate dissolution during the residual phase.

$$\frac{dC}{dt} = k_{rc}\frac{dL}{dt} \tag{2.22}$$

Cellulose degradation during residual delignification is pronounced compared to the other stages. This results in a lower yield and a reduction in pulp viscosity.

CHAPTER 3

METHODOLOGY

Although the movement of moisture into dry or unsaturated wood has been extensively studied[55-57], little is known about the diffusion of water into saturated wood. The purpose of these experiments is to examine how water behaves as it diffuses into saturated wood. There have been studies that examine how water transports into unsaturated wood by monitoring the weight increase in the sample. The sample is initially dry and is then placed in a high humidity chamber where the gain of water in the wood is gravimetrically determined. This is not possible when wood is completely saturated.

The transport of pulping chemicals and additives into water-saturated wood is key to efficient pulping [58], and the diffusion rates of sodium hydroxide have been reported [59, 60]. Factors such as tortuosity, size exclusion, and charge exclusion can all influence the kinetics of uptake. The rate of diffusion of water into saturated wood is a reference point against which the uptake of other compounds could be benchmarked. The use of tritiated water (HTO) allows such a measurement to be made, and similar techniques are commonly used in the study of sediments, soils, and membranes [61, 62]. Tritiated water is a conservative tracer for water; *i.e.* it moves with water and can be used to track water flow. It has been extensively used for this purpose in hydrogeology and other fields [63-65]. However, in these experiments deuterated water was tried first because it did not involve the use of radioactive materials.

3.1 Deuterium Experiments

3.1.1 Wood Preparation

The wood was kiln dried southern pine. It was disintegrated using a circular saw and the particles collected. The wood particles were then separated using Tyler screens on a shaking instrument. The wood particles were small, and the sieve sizes and configuration are listed in Table 3-1.

Table 3-1 Tyler Sieve sizes

Top	Sieve opening (mm)
	1.00
	0.850
	0.710
	0.600
	0.425
	0.250
Bottom	0.180

For a given experiment, one size fraction was taken and soaked in deionized water for 24 hours. The particles were ready once all descended to the bottom. The particles were then placed on a Buchner funnel and filtered. The filtered particles were placed in an airtight container. Experiments were conducted shortly after filtering off the excess water so as to minimize water loss due to evaporation. The moisture content of the wood was determined for all experiments.

3.1.2 Experiment Procedure

The wet wood particles were weighed and put into a reaction bottle. Typically twenty grams of wet wood were used per experiment. Five grams of 90 percent deuterated water

from Aldrich Chemical Co. was mixed with thirty grams of deionized water. The diluted deuterated water solution was poured into the Pyrex container holding the wood particles. One hundred microliter samples were extracted at various time intervals. The samples were placed into 2 mL GC vials. It was expected that the deuterium content of the bulk solution would decrease with time as the water diffused into the wood particles and exchanged with the wood moisture.

To determine the amount of deuterium in the samples, it was necessary to process the samples further. Added to the samples was 100 microliters of 2 N NaOH and a small amount of 2-butanone. 2-Butanone, also called methyl ethyl ketone, undergoes base-catalyzed enolization under these conditions[66]. The structure of 2-butanone is shown in Figure 3-1.

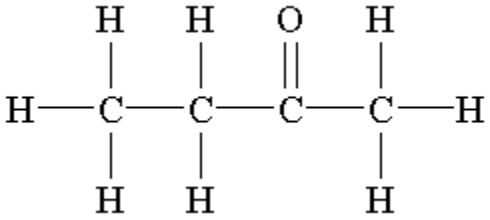

Figure 3-1 Chemical Structure of 2-butanone

The hydrogen atoms attached to the carbon atoms adjacent to the carbonyl group are available for exchange with the deuterium in the bulk solution. The reaction is fast[67, 68], but to ensure completion, the samples were placed in a hot water bath at 60 degrees

Celsius for one hour. The extent of the exchange was expected to be proportional to the percentage of deuterium in the sample.

To examine the amount of deuterium that had exchanged with protium, the butanone was run through a gas chromatograph coupled to a mass spectrometer (GC-MS). The sample containing the butanone was put in contact with a SPME fiber. SPME stands for Solid Phase Microextraction and is an assembly that allows for molecules to adsorb to the surface of the fiber. The fiber is then injected into the gas chromatography inlet port and the sample is run. The 2-butanone adsorbs well to the Divinylbenzene/Carboxen/Polydimethylsiloxane coated SPME fiber.

For analysis, the peak area located between 70 and 78 is examined. 2-Butanone, with a molecular weight of 72, would have a maximum molecular weight of 77 if all of the available hydrogen atoms were exchanged with deuterium not including the natural occurring isotopes of oxygen and carbon. To determine the precise amount of deuterium on butanone, the signals from the mass spectrometer detector are translated into abundances of the multi labeled molecules. These quantities would then have to be adjusted for the natural isotopes as well as the M-1 peak. The M-1 peak is small for butanone, and arises when a hydrogen ion is stripped from the molecule, located on the graph above at an m/z of 71. The percent deuterium labeled was calculated according to the formula derived for determining isotope composition for labeled compounds[69].

3.1.3 Results

The results were poor. After some investigation, it was found that an M-2 peak was occurring. The deuterium atoms were being split off instead of the hydrogen atoms. This made using the isotope calculations developed by Biemann[69] almost impossible. Still, a relative value of percent labeled could be calculated and compared to the other samples. Initially, samples were taken at long time periods, based on the assumption that diffusion would be slow. However, equilibrium was reached quickly and diffusion was occurring before the first sample point. The experiment was repeated and the sampling frequency was increased. Figure 3-2 is the result of the experiment.

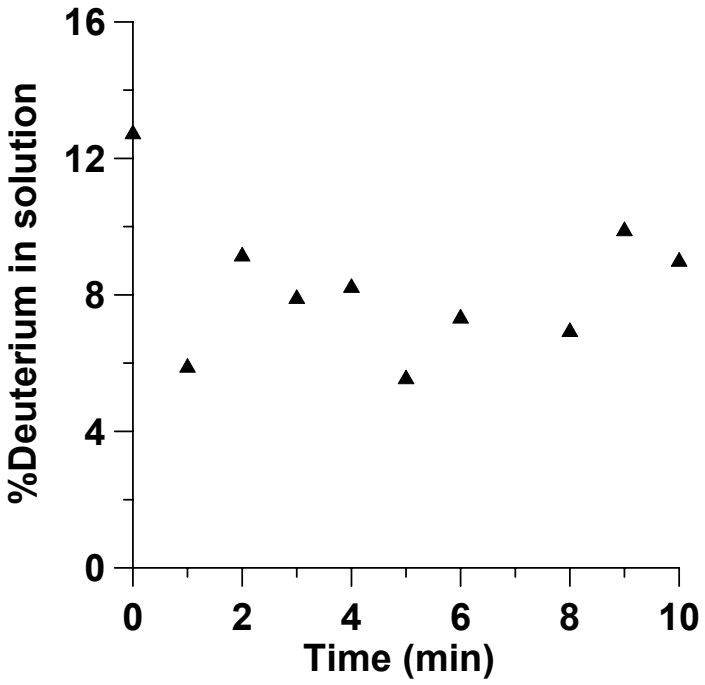

Figure 3-2 Deuterated water diffusion into wood particles as measured with GC/MS

These results were certainly not expected. There considerable scatter in the data for the short time sample points. Also, some data points are below the equilibrium for the long time experiments. This clearly can not happen.

The method of isotope exchange is not suited for deuterium. The equations used to calculate isotope composition do not work when the labeled compound is producing an M-2 peak. An alternative method is to eliminate the possibility of the deuterium being split off by reducing the power of the ionization[69]. However, this was not possible on our instrument.

3.2 Tritium Experiments

The wood used in these experiments was southern pine (*Pinus taeda*) from the Georgia Pacific particle board plant in Vienna, GA. The wood had just been cut and shipped to the mill and had never been dried. The particles were packaged and taken to the lab. Aspen (*Populus tremuloides*) chips from Alberta, Canada were obtained from Millar Western and then processed into small particles in a Wiley mill. The particles were then fractionated using multiple Tyler sieves mounted to an automated shaker. Each run of particles was on the screens for ten minutes. The screens were emptied and the particles were put into separate containers. The sizes of screens ranged from openings of 4.0 mm to 0.6 mm. Once separated, the wood was kept in airtight containers in a freezer until used for experiments. The sieve sizes and configuration are listed in Table 3-2.

Table 3-2 Tyler sieve sizes and arrangement for tritium experiments

Top	Sieve opening (mm)
	4.00
	3.35
	2.80
	2.35
	2.00
	1.70
	1.40
	1.00
	0.85
Bottom	0.60

The particles used in an experiment were first soaked in deionized water and stirred for at least 24 hours. The particles eventually sank indicating that they were water saturated. The soaking was followed up by a series of washes to get rid of any particulate matter or extractives that had diffused out of the wood. Once washed, the particles were filtered on a Buchner funnel to remove the excess water. The wet wood particles were then weighed out and placed in airtight Pyrex vessels. Experiments were completed shortly after filtering to minimize moisture loss from the wood. Moisture content was measured on a sample of the wet wood.

The experiment began when a pre-measured aliquot of tritiated water was combined with the wet wood. 100 Microliter samples were removed with a fixed volume pipette. The samples were place in scintillation vials with 10 mL of Scintiverse E scintillation cocktail. Samples were then run in a scintillation counter. The tritiated water added to the wood was first sampled to give a theoretical time zero data point. Initially samples were taken at pre-determined times, usually every minute. A stopwatch was used to monitor the experiment time and the moment to extract a sample. Later, it was

determined that the samples needed to be taken much more rapidly. Thus, samples were removed almost immediately after the tritiated water and wet wood were mixed. Samples were then taken as fast as possible.

The time to reach equilibrium turned out to be of the order of a few minutes. Once the tritium reached the expected equilibrium, more samples were taken to check that it was indeed at equilibrium and no more tritiated water was diffusing into the wood particles. For some of the particles, the reaction vessel would be sealed for 24 hours after the experiment. Then the excess tritiated water would be filtered off, and a fresh aliquot of deionized water introduced to the wood particles that were now equilibrated with tritiated water. The diffusion of tritiated water out of the particles was then monitored. Samples were taken in the same manner as explained for the diffusion into the particles.

3.2.1 Scintillation counter and radioactivity

A scintillation counter is a device that indirectly measures radioactive decay. A radioactive sample must be combined with a scintillation cocktail. A scintillation cocktail contains a solvent, an emulsifier, and a fluor. When a beta particle is emitted during tritium decay, the scintillation cocktail converts the beta particle into light which is detected by the counter. The conversion of a beta particle into light via the scintillation cocktail is illustrated below[70].

Step 1. Beta particle + Solvent → Solvent*

Step 2. Solvent* + Solvent → Solvent + Solvent*

Step 3. Solvent* + Fluor → Solvent + Fluor*

Step 4. Fluor* → Fluor +Light

* - denotes excited molecule

Once the beta particle excites the solvent molecule, chances are it will interact with another solvent particle before eventually exciting a fluor molecule. The excited fluor molecule then emits light as it returns to its ground state. The amount of light being emitted is proportional to the energy of the particle. The light is directed to photomultiplier tubes which converts it to a measurable electric pulse. Thus the scintillation counter can then give the results in counts per minute format.

Not all of the radioactive decay is detected by the scintillation counter. There are factors that reduce the amount of light that hits the face of the photomultiplier tubes. This phenomenon is known as quenching. There are two major ways a sample is quenched. Chemical quenching occurs when the energy from the beta particle does not make it to the fluor. This occurs when compounds such as water or oxygen interfere with the energy transfer from either beta particle to solvent, solvent to solvent, or solvent to fluor. The end result is that not as much light is produced. Weak chemical quenching agents are water and alcohol, but stronger ones are phenols and acetone.

Color quenching occurs when compounds absorb the light emitted from the fluor. The amount of absorption depends on the concentration and color of the quenching agent. Blue solutions slightly color quench, but yellow solutions will quench heavily. Color and

chemical quenching reduce the amount of light that hits the phototubes, thus less counts are recorded by scintillation counter.

All laboratory samples are quenched to some degree, so to allow for comparison of different quenched samples, the counts per minute(CPM) must be transformed into a number that describes the actual radioactive decay in the sample otherwise referred to as the disintegrations per minute(DPM). The CPM is related to the DPM by the counting efficiency as in Equation 3.1.

$$Counting\ Efficiency = \frac{CPM\,(events\ observed\ by\ instrument)}{DPM\,(actual\ disintegrations\ that\ occured)} \tag{3.1}$$

Counting efficiencies are determined from a quench curve. A quench curve returns a counting efficiency at known levels of quench. For the Beckman LS 5801 liquid scintillation counter used at IPST, the value of quench is given as an H-number, and using a quench curve the counting efficiency could be determined. The determination of an H-number for determining quench was developed by Beckman Instruments, primarily by Dr. Donald Horrocks[71]. The process of determining the H-number is complex, but is performed by the instrument and involves using an internal cesium source that determines the total quench of each sample.

3.2.2 Particle Analysis

The dimension and shape of a particle is important in modeling diffusion in that system. Initially, the particles were to be modeled as spheres, with a radius of the average of the Tyler sieves it fell between. For example, particles that fell through the 1.7 mm hole sieve but were retained on the 1.4 mm hole sieve would have a diameter of 1.55 mm. This was a poor assumption; several attempts at modeling the particles as spheres resulted in erroneous model outcomes. It was also clear that the particles were more like cylinders than spheres. In addition, simply averaging the sieve hole sizes to get a diameter of the particle had to be verified.

For a given particle size range, the particle would be spread out on a white background and painstakingly separated so that no particles were overlapping. For each particle size range at least 100 particles would be catalogued. The particles were then photographed with an Olympus C03030 digital camera. Figure 3-3 is an example of the particles for sieve size range 2.0 mm to 2.4 mm.

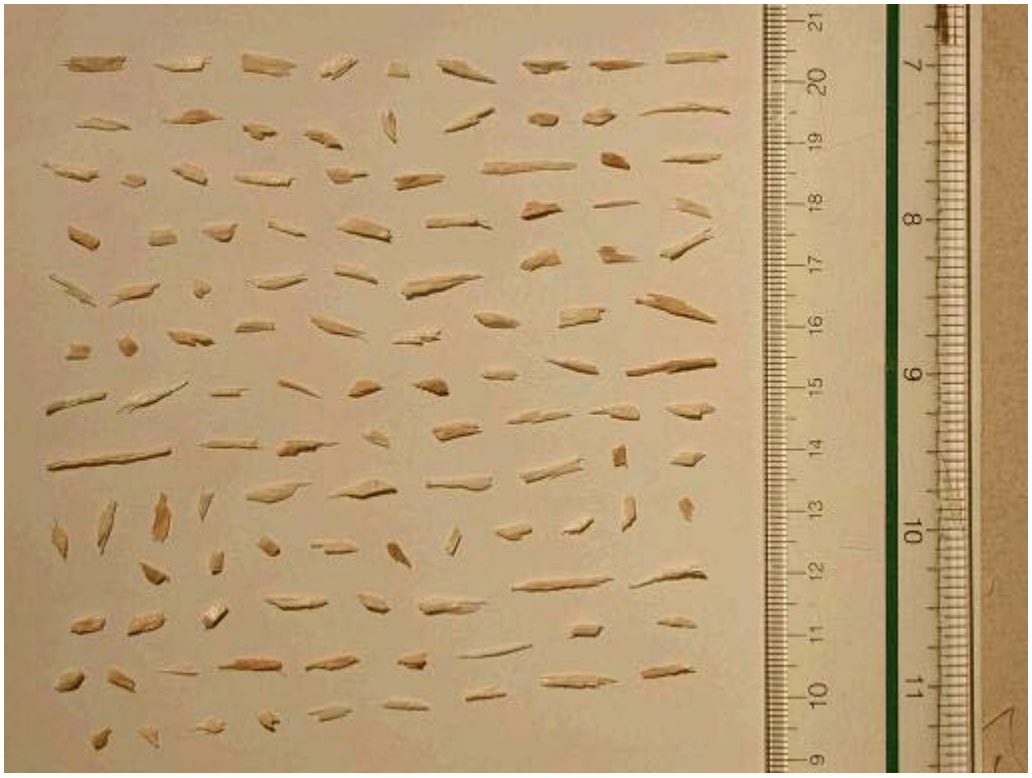

Figure 3-3 Digital image of wood particles used in particle analysis

The image of a ruler was captured in every photograph so that later the scale for each image could be set.

The particles were analyzed using a program called ImageJ version 1.32j[72]. This software was developed by the National Institute of Health and is a public domain image analysis software package. The original picture would be uploaded into the ImageJ program. To set the scale of the image, a line was drawn on the ruler that extended from the 10cm mark to the 20 cm mark. The option "set scale" was selected and the length of the line in pixels was displayed. The length and the units of measurement and the scale were then set for that photograph. The scale was similar for different images, but needed to be done each time an image was analyzed. Once the scale was set, the image needed

to be converted to an 8-bit grayscale image. The image then underwent a threshold procedure to clearly define items of interest and background. Figure 3-4 is a picture of what the previous image was transformed into.

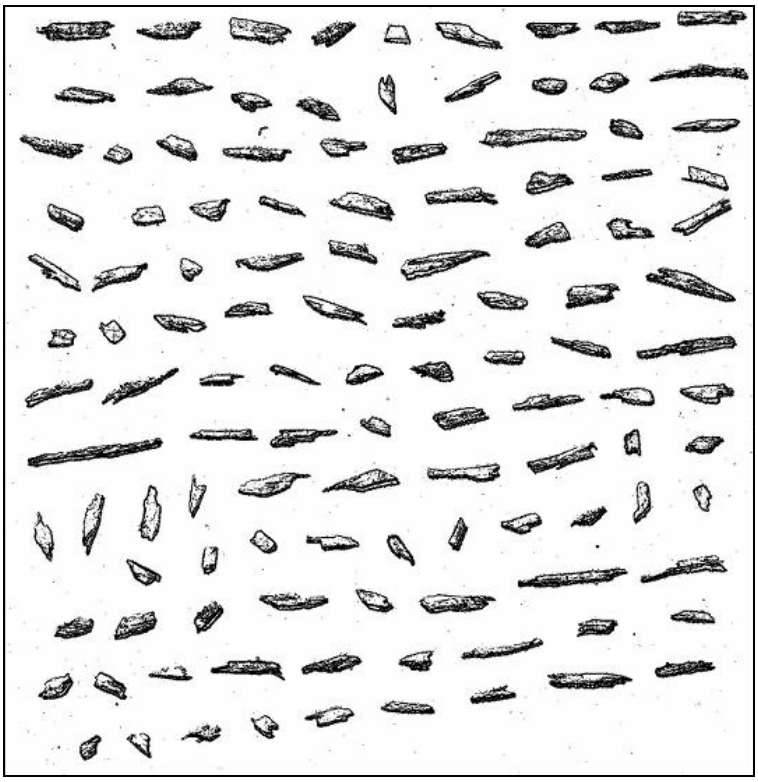

Figure 3-4 Picture of wood particles after converting to an 8-bit threshold image necessary for particle analysis program

The particle area would be selected and the function "analyze particles" would be started next. Limits would be set to exclude particles that did not meet a certain size. Sometimes in the image converting process, small spots would appear in the image that did not reflect a wood particle. These were eliminated from calculations by the minimum size exclusion parameter. ImageJ would then return the measurements of all the particles in the selected image area. The measured values were count, area, feret, major and minor ellipse measurements, and perimeter. The feret diameter is the longest distance between

any two points along the selection boundary. The major and minor ellipse measurements were derived from a best fit ellipse that is imposed on each particle, and the results are for the long and short axis. The method finally chosen to determine the length and the width for each particle was to use the feret diameter as the length, and for the width take the area divided by feret diameter of the particle. This was much closer to the actual dimension compared to the minor ellipse axis and verified by hand measurement. The measurements were averaged and in the case for the 2.0-2.4 mm particles, the length was 8.5 mm and the width was 1.86 mm.

Another point that needed to be checked was whether the average of the dimensions was representative of the sample. The values were separated into bins and Figure 3-5 shows the distribution of width measurements for the 2.0 – 2.4 mm particles.

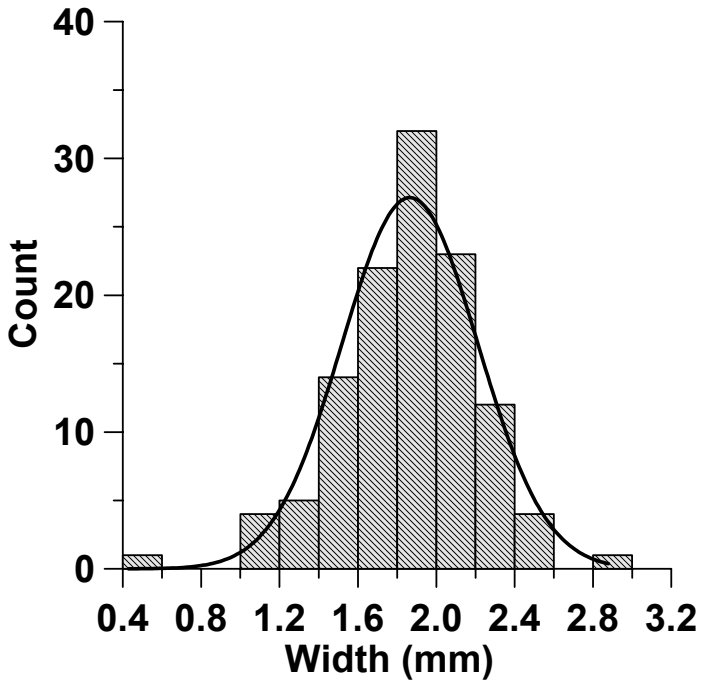

Figure 3-5 Histogram of width measurements of 2.0 – 2.4 mm size particles

Now the length and width were determined for the particle size range, but the thickness could not be measured in a 2-dimensional image. The particles that were imaged were now hand measured with a hand caliper. The results were compiled, and for the 2.0-2.4 mm aspen wood particles, their hand-measured thickness was 0.644 mm. This was also tested to determine the distribution of measurements. Results are in Figure 3-6.

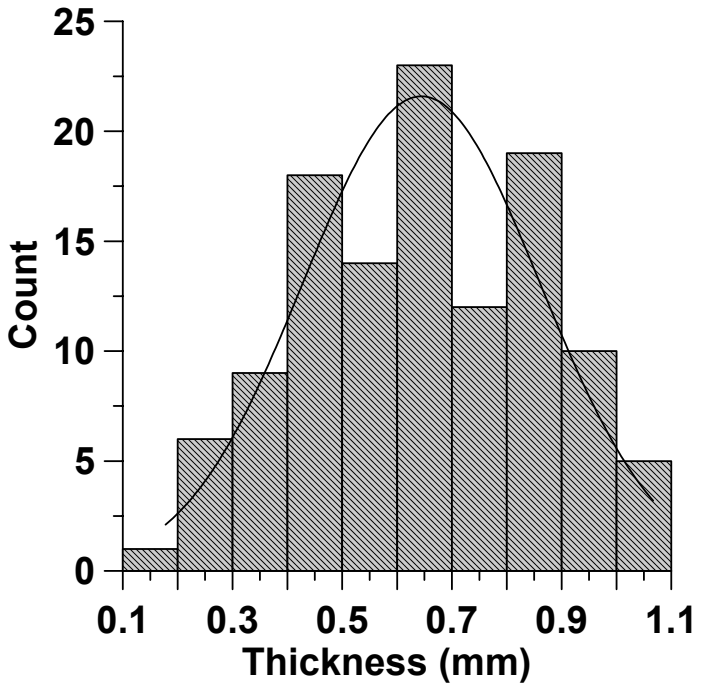

Figure 3-6 Histogram of thickness measurements of 2.0 – 2.4 mm size particles

Now a model could be constructed for what an average particle looked like for each particle size. The next step would be to determine the dimensions of an equivalent cylinder for each size range. A similar approach was taken in analogous experiments using a mixture of particles of different shapes and sizes[73]. The cylinder would have the same length as the measured particle. The radius would be determined by closely

fitting the penetration characteristics of the cylinder to the actual particle dimensions. This was accomplished by setting an arbitrary penetration length step. It was set low so as to get several points for each particle; in most cases it was set at 0.01 mm. For each step, the cylinder and model particle would be penetrated in all directions by the penetration step length. Then a percent volume penetration could be calculated for each particle at each step length. The step length was taken until both particles were 100% penetrated. At each penetration length, the difference of percent volume penetrated was calculated between the cylinder and particle model. The differences were squared and then summed. The solver program was used to set the sum of squares to a minimum by changing the value of the cylinder radius. The end result is depicted graphically in Figure 3-7 showing the penetration of both particles.

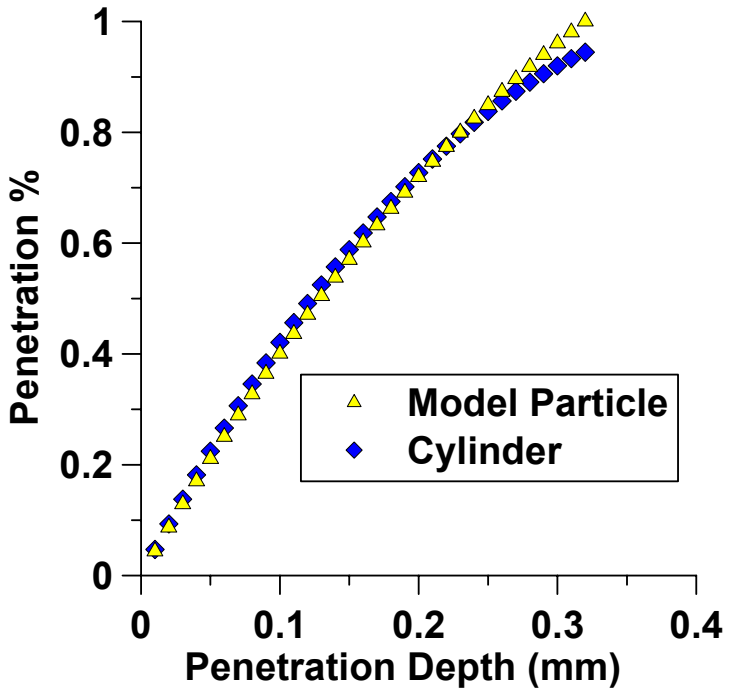

Figure 3-7 Graphical representation of penetration into a cylinder and the measured wood particles

Table 3-3 is a chart that summarizes the measurements of the particles used in the diffusion experiments.

Table 3-3 Summary of dimensions of all particles sizes and the corresponding cylinder radius used for modeling

Size Fraction (mm)	Actual Dimension (mm)			Effective Cylinder Radius (mm)
	Length	Width	Height	
Pine				
1.4 – 1.7	3.8	1.3	0.48	0.305
1.7 – 2.0	4.2	1.6	0.57	0.364
2.0 – 2.4	4.6	1.9	0.75	0.468
Aspen				
1.4 - 1.7	8.9	1.3	0.42	0.277
1.7 - 2.0	9.3	1.5	0.51	0.345
2.0 - 2.4	8.5	1.9	0.64	0.42

3.2.3 Data conversion

The scintillation counter returns the counts per minute (CPM) and the H-number for each sample. The decompositions per minute are calculated and plotted versus time. Figure 3-8 is an example of results from an experiment with 2.0-2.4 mm pine particles.

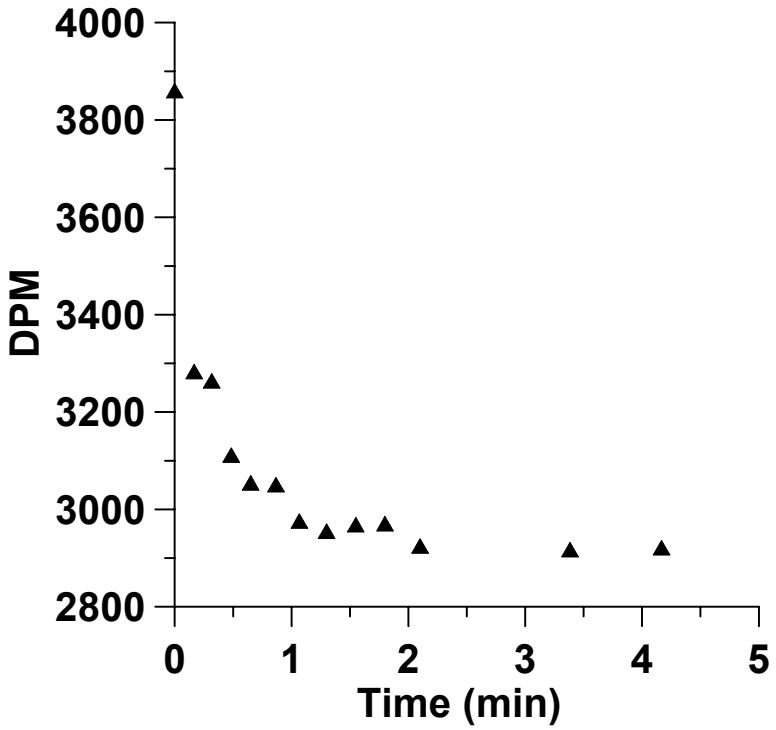

Figure 3-8 Decompositions per minute versus time for 2.0-2.4 mm pine particles

In this experiment, the decompositions per minute level off at two minutes at a value of 2914 dpm. A theoretical equilibrium can be calculated for each experiment. It is derived by taking the radioactivity (DPM) of the tritiated water before it is introduced to the wood and calculating the radioactivity (DPM) if it were simply diluted with the amount of water in the wood. The total amount of tritium will not decrease but the radioactivity per sample will. The theoretical DPM at completion is also called the equilibrium of mixing. In the case of the 2.0-2.4 mm particles, the equilibrium of mixing was 2917. This was within 1% of the measured equilibrium value. For all experiments the difference between the calculated equilibrium and the measured equilibrium was no greater then 2%.

Setting the equilibrium at an appropriate point is essential when the data is converted into reaction coordinates or M_t/M_∞ points. This is done according to equation 3.2.

$$\frac{M_t}{M_\infty} = 1 - \frac{DPM_t - DPM_{eq}}{DPM_0 - DPM_{eq}} \tag{3.2}$$

Where M_t = mass of tritium inside particle at time t

M_∞ = mass of tritium inside particle at infinite time

DPM_t = measured DPM at time t

DPM_{eq} = equilibrium of mixing

DPM_0 = DPM at time 0

Transforming the data in this way made it possible to insert the results into the diffusion equations. Now, all data points would either be between zero, the theoretical starting point, and 1, the equilibrium or end of experiment. Figure 3-9 shows the data for the 2.0-2.4 mm pine particles after transformation.

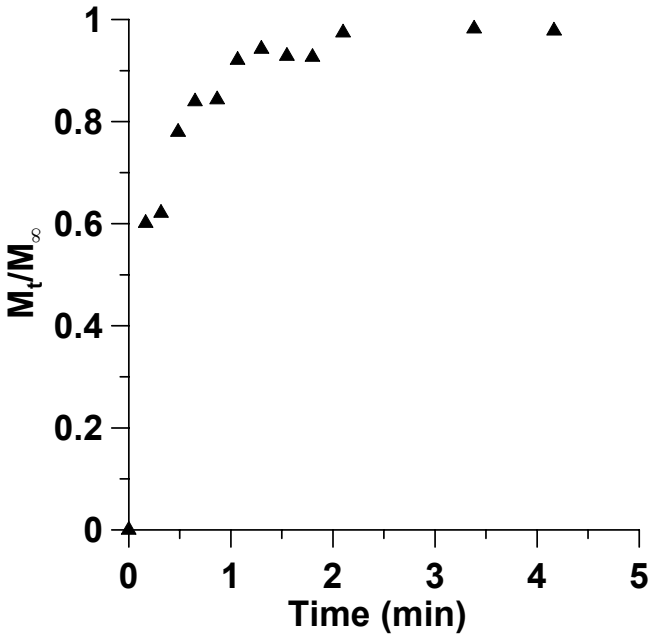

Figure 3-9 M_t/M_∞ versus time for 2.0-2.4 mm pine particles

3.2.4 Modeling

The aspect ratios of the particles suggested that they could be modeled as cylinders. Fick's second law describes mass transfer in cylindrical coordinates through Equation 3.3, where C_a

$$\frac{\partial C_a}{\partial t} = D_e\left[\frac{\partial^2 C_a}{\partial r^2} + \frac{1}{r}\frac{\partial C_a}{\partial r}\right] \tag{3.3}$$

represents the concentration of species *a*, D_e is the effective diffusion coefficient, *r* is the distance from the center axis of the cylinder, and *t* represents time. The boundary conditions are

$$C(a,t) = C_b(t); t > 0$$

$$C(r,t) = 0; 0 \le r \le a; t = 0$$

$$\frac{\partial C}{\partial r} = 0; r = 0, \textit{for all } t$$

If M_t and M_∞ are defined as the mass of solute inside the cylinder at time *t* and at infinity, respectively, then two solutions emerge, one for short periods where $M_t/M_\infty > 0.5$ and one for longer times [74]. This ratio can be thought of as a reaction coordinate since M_t/M_∞ is initially zero and reaches one at completion. Data points were all taken after $M_t/M_\infty > 0.5$ and only the solution for long times was used. This is given by Equation 3.4 where α_n's are the positive roots of the Bessel function of order zero. The variable *r* is the radius of the particle.

$$\frac{M_t}{M_\infty} = 1 - \sum_{n=1}^{\infty} \frac{4}{r^2 \alpha_n^2} \exp\left(-D_e \alpha_n^2 t\right) \tag{3.4}$$

Bessel functions are useful for solving differential equations in cylindrical coordinates. Figure 3-10 shows the zero and first-order Bessel functions and their derivatives plotted over various *x*[75]. The roots of the Bessel function of a certain order are the intercepts between the Bessel function curve and the *x* axis.

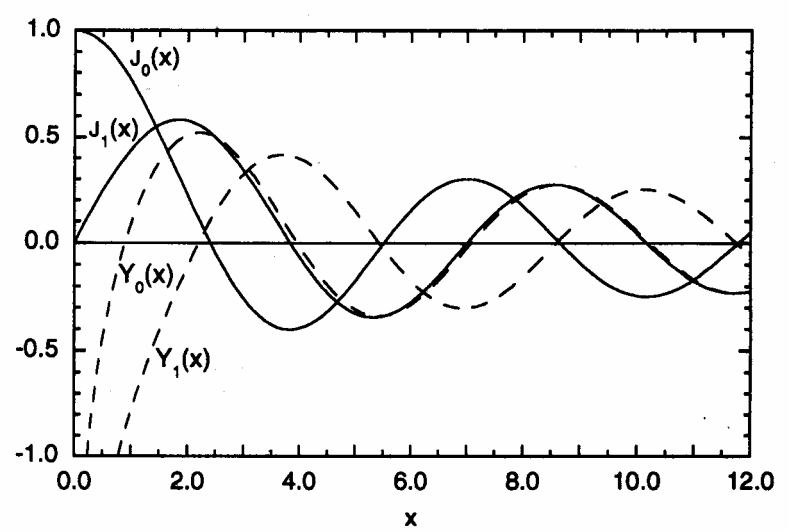

Figure 3-10 Graphical Representation of Zero and 1st Order Bessel Functions (J_0x) with Derivatives (Y_0x)

Table 3-4 shows the first five roots for the zero-order Bessel function are[76]:

Table 3-4 Roots for the Bessel function order zero

α_n	**Zero-Order**
1	2.405
2	5.52
3	8.654
4	11.792
5	14.931

Equation 3.4 was programmed into Excel, the summation was taken to the fifth term, beyond which the solution did not change with additional terms. A least squares approach was used to obtain the best fit of the model to the experimental data. Excel solver was used to minimize the residuals and an effective diffusion coefficient (D_e) was determined. Figure 3-11 shows the 2.0-2.4 mm pine particle data and the model results with the best fit diffusion coefficient.

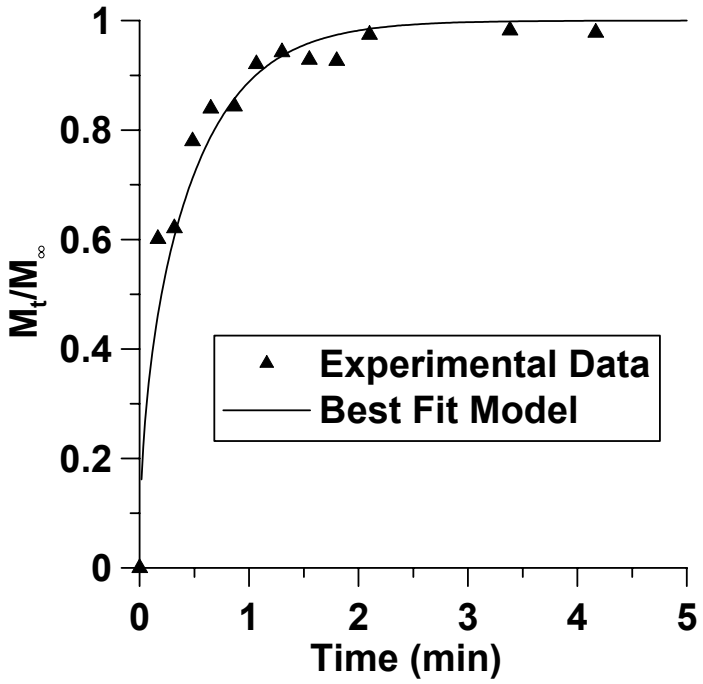

Figure 3-11 M_t/M_∞ versus time for 2.0-2.4 mm pine particles and model line using the best fit diffusion coefficient

The diffusion coefficient for this experiment is 1.27 x 10^{-5} cm^2/sec. This parameter is related to the porosity of the material (ε), the self-diffusion coefficient (D^o), and the tortuosity (τ) through Equation 3.5. The tortuosity is a dimensionless number that describes how the diffusion of a substance is impeded in a

$$D_e = \frac{\varepsilon}{\tau} D^\circ \tag{3.5}$$

material. It is sometimes referred to as a retardation factor [77]. Porosity is also a dimensionless number that represents the void fraction of a material where diffusing molecules can migrate.

3.3 Sulfide Experiments

In these experiments, sulfide in a white liquor solution was monitored as it diffused into wood particles. Softwood chips were acquired from the Georgia-Pacific Port Hudson, Louisiana mill through the Institute of Paper Science and Technology. These chips represent a random sample taken after the mill's screening process. They also represent a typical species mix, most likely with a majority of southern pine. The chips were sampled after the mill's slotted screens. They were stored in an air-tight bag in a cold room to prevent decay. The chips were inspected for rot and other deformations to ensure that they were fresh chips and therefore a representative sample.

The chips were then processed into small particles in a Wiley Mill. They were fractionated with multiple Tyler sieves mounted to an automated shaker and stored airtight in a cold room. The screen openings ranged from 0.6 to 4.0 mm. The particles were stirred in deionized water for at least 24 hours, at which point no floating material was observed. They were then washed at least ten times to remove any particulate matter or extractives that may have diffused out of the wood, filtered, and stored in airtight vessels. Experiments were completed shortly thereafter to minimize moisture loss from the wood.

A typical mill white liquor was used for every experiment. A goal of 100g/L of active alkali (AA) and 30% sulfidity was desired. Anhydrous sodium hydroxide (NaOH) was added to a tared one liter sample container. Sodium sulfide (Na_2S) was then added in a

similar fashion. Water was added to make the resulting solution one liter. A mixing rod was added and the solution was allowed to stir until the solids dissolved into solution. Since the Na_2S oxidizes in the presence of air, air-tight containers were used to keep the sulfidity stable.

The ABC (acid-base-carbonate) liquor test was used to determine the strength of the previously made white liquor. It was also used to measure the diffusion of sulfur into the chips. The ABC test used was an IPST modified test of TAPPI 624 cm-00 [78]. The white liquor container was placed on a magnetic stirrer and allowed to mix for 5 minutes while the titrator was calibrated.

A Mettler DL-21 titrator was used to perform the test. The DL-21 is an electronic titrator accurate to +/- 0.3% per titration. The titrator performs an acid-base titration and uses a pH probe to measure the sample. During the titration it adds 0.5N HCl to lower the pH to the desired set-point of 9.3. Once the set-point is reached, the titrator displays the amount of the 0.5N HCl used in mL.

By using the ABC test and the DL-21 titrator, diffusion into the softwood fragments could be measured. Tests were performed using several 100mL sample containers. Their shape resembled a standard commercial batch digester. The containers were completely air-tight and transparent to allow viewing of the liquor. First, the main container of wood fragments was removed from the cold room. A sample container was labeled and then placed dry on a balance and tared. A sample of fragments was then placed into the

sample container. Wet particles (6.67g, 2g OD) were used for each experiment. After the particles were placed into the container, the lid was replaced so that the particles remained at their saturated moisture level. Several more containers were filled (usually 6 to 8) and then placed into a rack for transport. The sample containers were then moved to the DL-21 titrator and allowed to reach room temperature. Next, the container of white liquor was placed on a magnetic stirrer to ensure a uniform mixture. The ABC test was then performed on the liquor to ensure that no oxidation had taken place and that the liquor was comparable to other experiments in the series. It was also used as the initial value in each experiment to measure the diffusion taking place. The white liquor was at room temperature for the test.

Several temporary glass containers were collected and tarred. White liquor was added to these containers based on weight (usually 20g). The white liquor containers were then placed next to the sample containers with fragments. A stopwatch was zeroed and then started as soon as the liquor was added. Each sample container was then sealed and the starting time recorded. A sample of the liquor is taken from the vessel at a predetermined time. The goal of running the ABC tests was to measure the diffusion of Na_2S into the size fractions used. Initially, all of the sampled particles reached equilibrium before the measurement was complete. As the measurement time frame shortened from hours to minutes to seconds, a clearer picture of the actual diffusion process developed, and measurements were taken before the particles reached equilibrium.

Particle analysis for the wood particles was done as described earlier for the tritiated water experiments. Data analysis and modeling was also used as described for the tritiated water experiments.

3.4 White Liquor Diffusion in Wood Chips

A second set of experiments was conducted to expand on the results from the diffusion experiments. Sweet gum hardwood chips that were never dried were impregnated in synthesized white and green liquor at 103°C for 5 to 25 minutes. The cooked chips were split into two pieces in the *z* direction. Indicator solutions were applied via a spray atomizer. One was stained with 1% phenolphthalein ethanol solution, whereas the other piece was stained with 3% silver nitrate solution adjusted to pH 3.00 with H_2SO_4. The images of stained woodchips were recorded with an Olympus C03030 camera. The difference in penetration speeds between hydrosulfide ion and hydroxide ion was visually evaluated by comparison of silver nitrate stained and phenolphthalein stained wood chips.

3.5 Pulping Experiments

Pulping experiments were done on chips and sawdust. The wood used in the experiments was either softwood or hardwood chips from the Port Hudson mill. The softwood mix was predominantly southern pine but the hardwood mix was relatively mixed. Due to this uncertainty, most of the hardwood cooks were conducted with Sweetgum chips that were taken from a tree cut down from a residence outside of Dublin, GA. Two four-foot sections taken near the base of the tree were transported to Georgia Tech where they were

debarked by hand, and then chipped. Debarking was done with a two-handed slit knife debarking instrument.

The addition of wood fines to the normal size chips was a focus in this study. Fines were shipped from the Port Hudson mill along with the chips. If more fines were necessary, they were produced on a Wiley mill. It was determined later that the wood fines should be separated by size. This was done on a series of Tyler sieves that were mounted to an automatic shaker.

Kraft pulping was used in the cooking of these wood chips and particles. Kraft cooking uses two primary chemicals, sodium hydroxide and sodium sulfide. Sodium hydroxide, 10 N from VWR, and solid sodium sulfide nonahydrate from Fisher Scientific were combined to make up the white liquor for each batch.

The cooks were done in a multi-digester apparatus manufactured by Aurora Technical Products Ltd. Each digester was individually controlled and heated. The whole apparatus would rotate through a 300 degree arc to mix the contents of the digester since there was no internal mixing via impellers or recirculation lines. The digesters had a volume of 1 L and a maximum load of 100 grams of oven dry wood. A thermocouple inside each digester connected to a control computer to monitor the temperature and extent of cook. The temperature and rate of temperature change could be changed depending on the experimental conditions.

After the target H factor was reached, the vessels were removed from the apparatus and quickly cooled to room temperature in a water bath. The chips were removed and disintegrated in a Waring blender. The pulp was washed and thickened and the wet weight and consistency measured to calculate the total yield. The washed pulp was stored in a refrigerator until additional tests were run. The kappa number of the pulp was measured according to TAPPI standard test methods.[79]. For some pulping runs a small sample of the black liquor would be kept. In those cases the black liquor solids were analyzed using the TAPPI method [80].

Table 3-5 shows the experimental conditions typical for each cook.

Table 3-5 Pulping conditions for kraft cooking of wood chips

	HW	**SW**
Wood charge (oven dry g)	100	100
AA% (Na_2O)	18	18
sulfidity %	30	30
L:W ratio	4	4
ramp time 25°C – 100°C (min)	30	30
ramp time 100°C – 170°C (min)	60	60
Temp ^oC	170	170
H-factor	600	1400

Table 3-5 contains the conditions for pulping wood chips. In the case where only sawdust was being pulped, the liquor to wood ratio would be increased to 6:1 due to the tendency of sawdust to soak up all the free liquor in the digester. The H-factor was also varied in a set of experiments to determine how the wood particles would propagate throughout the cook.

Sawdust pulping gives weaker sheets due to the decrease in fiber length. The fiber length of our pulps was measured using a Fiber Quality Analyzer (FQA). The amount of fines per cook was determined using a dynamic drainage Britt Jar according to TAPPI test method 261[81].

The diffusion experiments were done with wood particles that were much smaller than typical wood chips. To compare the diffusion results to kraft pulping, the same size wood particles were pulped. In addition, there was a study done in which it was shown that adding hardwood fines to a normal cook the amount of fiber fines would increase proportional to the amount of wood fines added[82]. In softwood cooks, it appeared that the increase in wood fines would not translate to an increase in fiber fines. To determine how cooking affected the wood fines, cooks of varying duration were conducted with chips and sawdust together. There was not enough hardwood fines from the mill so fines were produced on a Wiley mill and then passed through a 3mm hole screen.

CHAPTER 4

RESULTS AND DISCUSSION

4.1 Tritium Experiments

Results from measurements made for 2.0-2.4 mm particles are shown in Figure 4-1 from which an effective diffusion coefficient of water of 1.0 x 10^{-5} cm^2 s^{-1} is obtained.

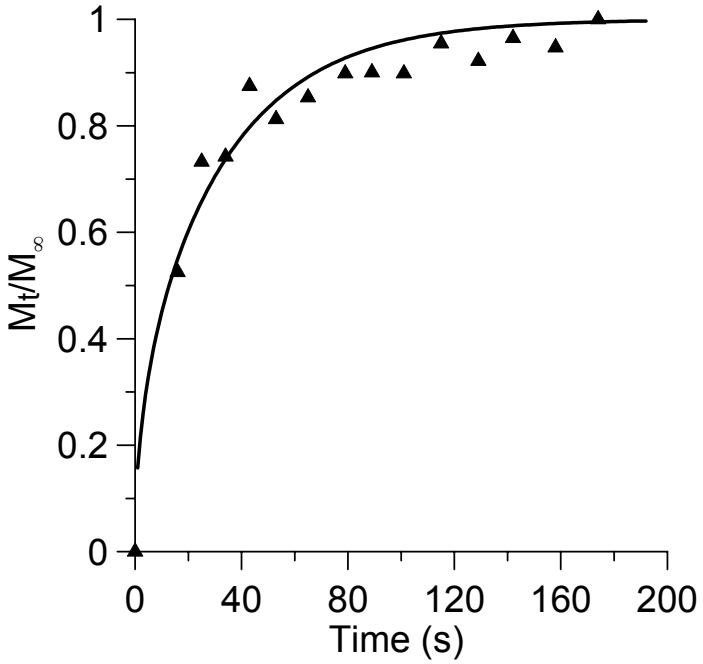

Figure 4-1 Diffusion for 2.0-2.4 mm pine particles

Use of 2.5 x 10^{-5} cm^2 s^{-1} as the self-diffusion coefficient of water at 25^oC [83, 84], and a porosity of 0.69 for pine [85] leads to a tortuosity of 1.6. In other words the diffusion of water into these saturated particles will only be about 40% slower than the diffusion of water in water itself.

One of the major assumptions in this work is that the diffusion of tritiated water into saturated wood follows Fickian mechanics. Fickian diffusion requires a plot of 1 - M_t/M_∞ to be linear with for $M_t/M_\infty > 0.5$. An example of tritium diffusing into pine particles is shown in Figure 4-2.

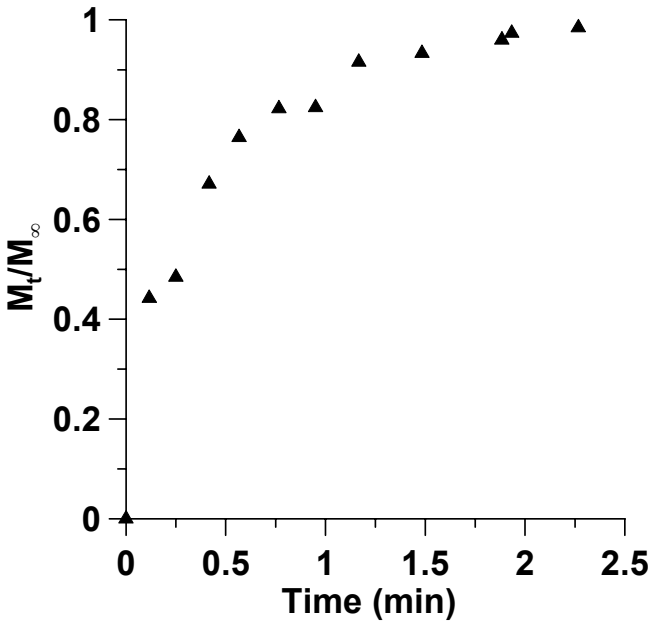

Figure 4-2 Diffusion into pine particles

The test for Fickian diffusion is shown in Figure 4-3.

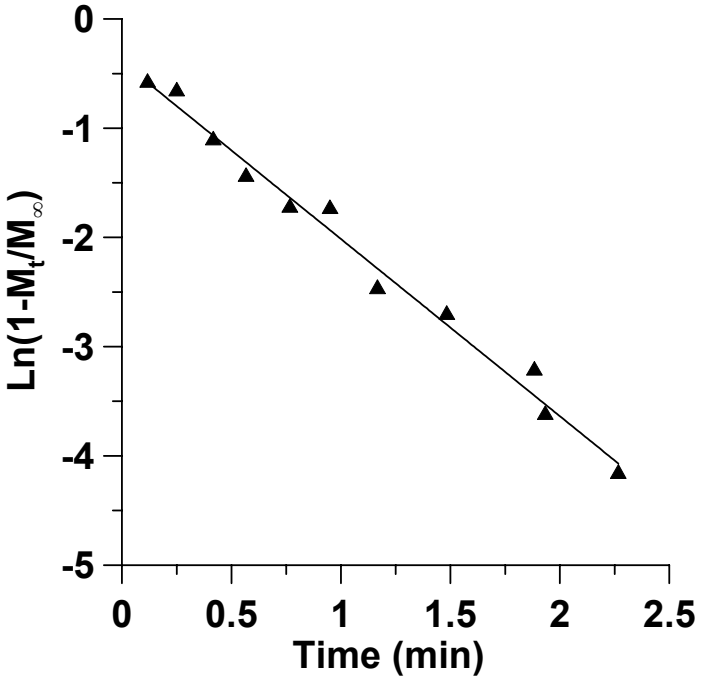

Figure 4-3 Test for Fickian diffusion using pine data

The R^2 value for this experiment was 0.986. This degree of linearity was typical for all the experiments.

For aspen, the diffusion into and out of the particles was nearly identical, demonstrating that diffusion of water into saturated wood particles is completely reversible. There was no hysteresis for the saturated wood as is common for water adsorption into unsaturated wood. Therefore, all the regions in fully saturated wood are equally accessible to the diffusing water molecules. Water that is highly bound to the wood structure readily exchanges with the loosely bound bulk water. Figure 4-4 shows the diffusion into and out of 2.0-2.4 mm aspen particles.

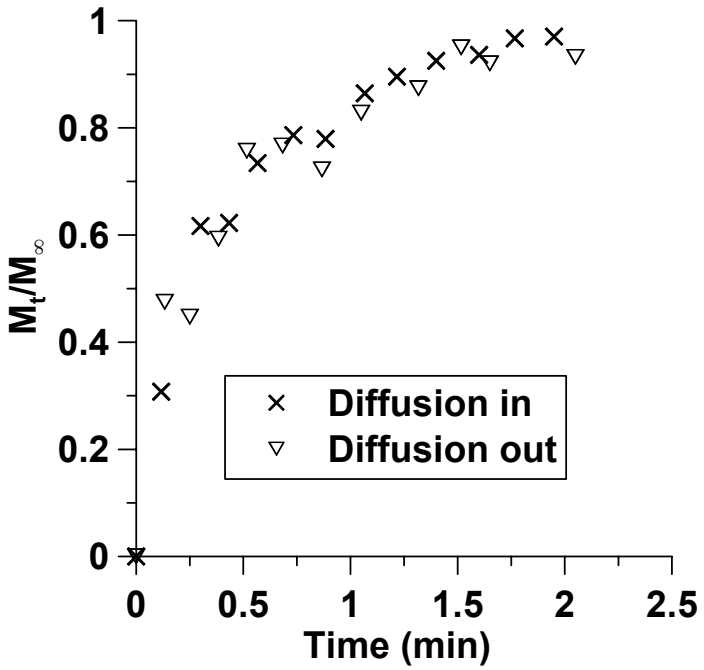

Figure 4-4 Diffusion into and out of 2.0-2.4 mm aspen particles

The calculated diffusion coefficient for the tritiated water transporting into wood particles of this size is 7.7 x 10^{-6} cm^2/s. The diffusion coefficient for the tritiated water transporting out of the same particles is 8.1 x 10^{-6} cm^2/s.

Experiments were also conducted on 1.7-2.0 mm pine particles at different temperatures. Figure 4-5 shows the experimental data as well as the best fit model.

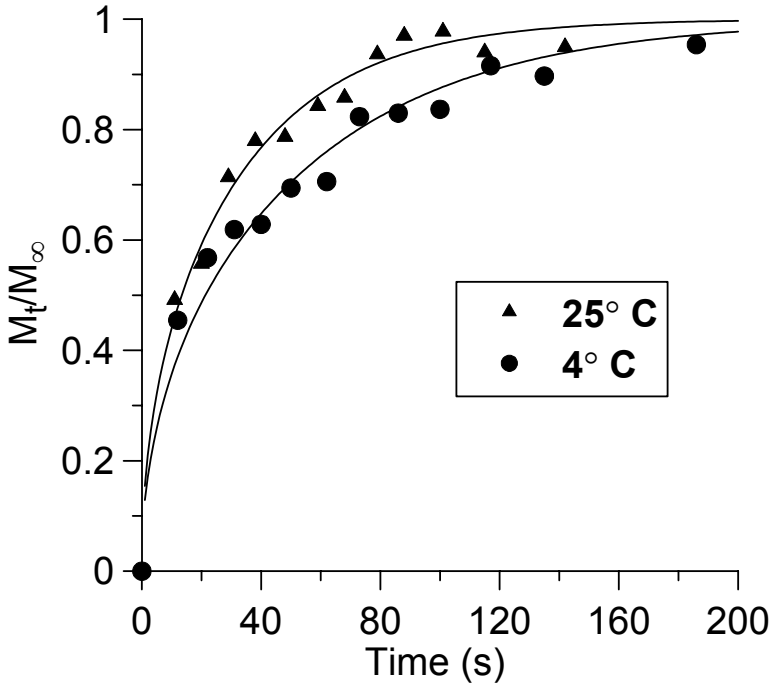

Figure 4-5 Diffusion into 1.7-2.0 mm pine particles at two temperatures

If an Arrhenius relationship is assumed, then an activation energy of 21.7 kJ/mol results. This is in good agreement with published values of 20 kJ/mol [86]and 20.5 kJ/mol [83] for the self diffusion of water. As expected, the tortuosity remains unchanged with temperature.

Diffusion parameters for pine and aspen particles are summarized in Table 4-1.

Table 4-1 Summary of results for tritiated water experiments

Size fraction (mm)	Direction	Temperature (^{o}C)	D_{eff} x 10^{6} cm^{2} s^{-1}, (σ)	Tortuosity
Pine				
2.0 - 2.4	In	25	11.1 (0.5)	1.6
1.7 - 2.0	In	25	6.8 (0.8)	2.5
1.7 - 2.0	In	4	3.5 (0.5)	2.2
1.4 - 1.7	In	25	6.0 (0.9)	2.9
Aspen				
2.0 - 2.4	In	25	7.2 (2.8)	3
2.0 - 2.4	Out	25	8.3 (1.4)	2.4
1.7 - 2.0	In	25	4.9 (1.2)	4.1
1.7 - 2.0	Out	25	4.9 (1.2)	4.1
1.4 - 1.7	In	25	3.1 (1.2)	6.8
1.4 - 1.7	Out	25	2.9 (0.3)	6.6

The tortuosity values are illustrated in Figure 4-6.

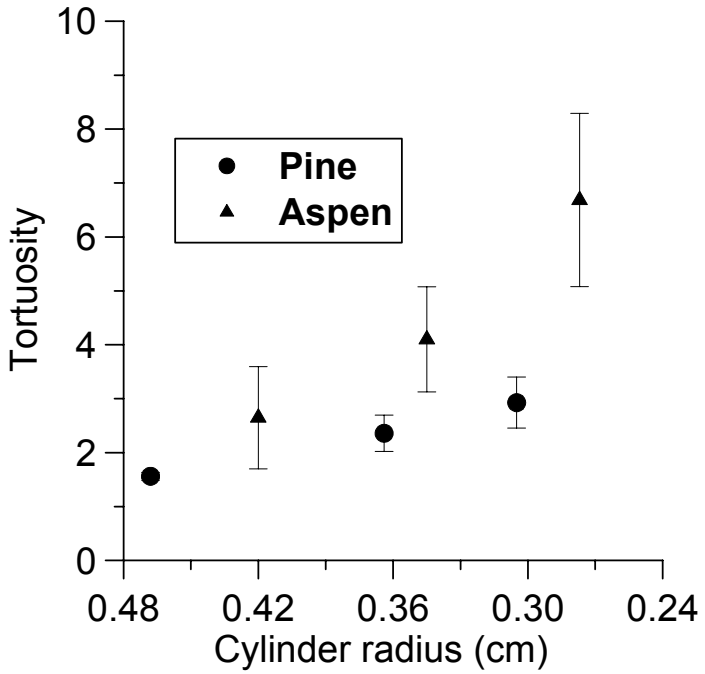

Figure 4-6 Tortuosity of pine and aspen particles versus particle cylinder radius

The tortuosity is higher for hardwood than for softwood particles, probably because the hardwood fibers are much shorter. In addition to fiber length differences, hardwoods also have a more diverse composition of structures that will facilitate mass transport. *Pinus taeda* is primarily composed of wood fibers, approximately 91% by volume [85]. The remaining percentage is mostly rays with a small percentage occupied by resin canals. *Populus tremuloides* is approximately 55% wood fibers, 34% vessel elements, and 11% rays[87]. The vessel elements in hardwood should help increase diffusion, but these structures may not be fully intact in wood that has been processed into small particles. It is significant that the tortuosity decreases with increasing particles size for both hardwood and softwood. In other words, as the wood particles increase in size, the relative resistance to diffusion decreases.

Our observation of increasing tortuosity with decreasing particle size has been reported in other areas. Cadmium uptake into chitosan particles showed a similar relationship [88]. The authors suggest that although they modeled the chitosan particles as spheres, the larger particles were actually flat discs, which would increase the uptake efficiency and would be reflected in the tortuosity factor. The sulfation reaction on different limestone sorbents also showed that tortuosity increased as the particle size decreased[89]. This occurred only for limestone particles with a unimodal pore size distribution. Particles with a wider distribution showed no change in tortuosity with changing particle size. The authors speculate that the increase in tortuosity for smaller particles may be due to variations in porosity.

It should be pointed out that even though the smaller particles restricted diffusion more, the overall mass transfer is still faster for smaller particles. Figure 4-7 shows two size ranges of aspen particles.

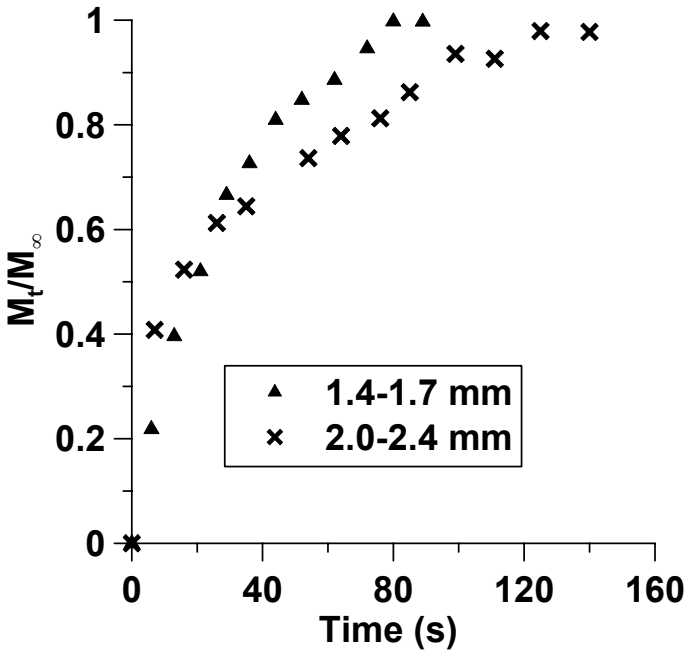

Figure 4-7 Diffusion into two sizes of Aspen particles

The smaller aspen particles clearly reach equilibrium faster than the larger particles. However, when these results are put into the diffusion model, the size of the particles is taken into account. This is where a difference appears, diffusion of tritiated water into the smaller particles should be faster than what was observed.

It is possible that the movement of tritium into the system could occur through proton transfer rather through the movement of the tagged water molecule. If this were the case, then the diffusion coefficient would have been much larger than that typical for water. The self-diffusion coefficient of HDO, HTO, and $H_2{}^{18}O$ at 25°C are all nearly identical [83]. If proton transfer were significant, there would be appreciable differences among these coefficients.

Figure 4-6 shows that the hardwood tortuosity increases to a greater extent than that of softwood with decreasing particle size. The reasons for this difference are not understood, but tortuosity would increase if pore closure occurred while the particles were being cut. Hardwood fibers are shorter in length and smaller in diameter than their softwood counterparts [87], and the tortuosity of hardwood could, therefore, be more sensitive to pore closure.

The diffusion of water into saturated materials has been extensively studied. Both wood and soil have capillary flow channels. In soils, there are large pathways between soil aggregates that allow for flow and non-restricted diffusion, and also small pathways where diffusion is restricted due to small openings and tortuous pathways [90]. Tortuosity values from several types of soils are similar to those for wood. Fully saturated Bentonite sand mixtures have tortuosities of 1.5 to 3 [91]; those for 1.4-1.7 mm and 1.7-2.0 mm wood particles are 2.7 and 1.9, respectively. Experiments done on lake sediments yielded lower tortuosity values, ranging from 1.1 to 2 [92].

The diffusion of tritiated water and [^{36}Cl] calcium chloride into porous ceramic spheres has been studied [93]. The spheres are aggregated media with distinct mobile and stagnant pore water regions. The effective diffusion coefficients of the tagged chloride ion and the tritiated water were the same. However, this leads to the tritiated water having a higher tortuosity value than the chloride ion. We calculated tortuosities of 1.2 and 2.7 for water and chloride, respectively. Neither the tritiated water nor the chloride

ion was adsorbed onto the ceramic material. In soils, charge exclusion becomes a factor in transport of materials and this may be the case in wood also.

There was no apparent difference between diffusion into bound water and into free water, *i.e.* the diffusion coefficients remained constant throughout the process. This differs from the isothermal adsorption of the water vapor into dry wood [94], where Fick's law is not obeyed, since the diffusion coefficient changes as wood picks up more moisture. Also, in similar diffusion experiments in soil, there was not a fraction of water that could not be diffused into [77].

The lower tortuosity of pine versus aspen may have applications in pulping and wood drying. Uniform chips are required for consistent pulping; small chips tend to overcook. However, the tortuosity of aspen chips increase with decreasing chip size, which will tend to somewhat offset the size effect. In the drying of sapwood boards, liquid flow is significant [95], and is analogous to diffusion in that the flow will primarily follow the same tortuous pathways through which water diffuses into wood. Although wood drying is affected by many variables, the more tortuous path in aspen will make drying more difficult in the initial and constant rate regime, as is the case for most hardwoods compared with softwoods [96].

4.2 Sulfide Diffusion results

As mentioned earlier, the sulfide diffusion reached equilibrium rapidly. Figure 4-8 is an example of how the sulfide diffused into the 3.35 – 4.0 mm particles.

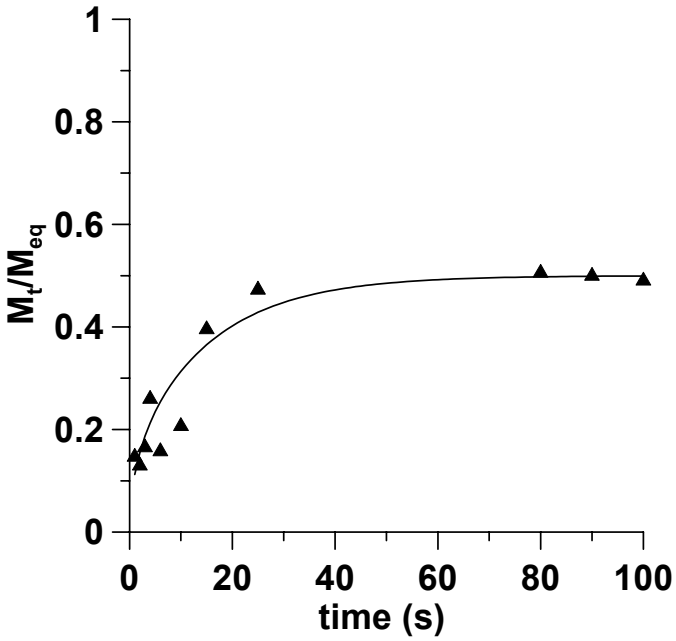

Figure 4-8 Sulfide diffusion into 3.36 – 4.0 pine particles

The M_t/M_{eq} is the ratio of the amount of sulfide diffused into wood at time *t* compared to the quantity expected if equilibrium was reached, *i.e.* if the sulfide was able to access all the water in the wood. In other words, the M_{eq} value would be obtained if the concentration of sulfide in wood water was the same as that in the bulk water. Note that the diffusion rate levels off well below the equilibrium value. This contrasts with our previous results with tritiated water where the curve leveled off at the equilibrium value. Hence, the Figure 4-8 result suggests that the sulfide is not able to access all the water in wood, *i.e.* there are large regions in wood from which sulfide is excluded.

Results for the effective diffusion coefficient and the tortuosity are provided in Table 4-2 and show that the apparent tortuosity of sulfide is less than one.

Table 4-2 Apparent tortuosity of sulfide diffusion into wood particles

Size Fraction	Radius	D_e	Std. Dev.	Apparent Tortuosity	
(mm)	(mm)	X 10^{-5} cm^2 s^{-1}	σ	HS^-	S^{2-}
3.36 – 4.0	0.76	5.73	0.80	0.21	0.31

The tortuosity of a porous solid can be expressed as the actual diffusion path length divided by the diffusion path length if there were no solid material present. By this definition, it is impossible to obtain a tortuosity of less than one. Previously, we found that the effective diffusion for tritiated water into 2.0-2.4 mm size pine particles at 25 ºC was 1.11 x 10^{-5} cm^2 s^{-1} and the resulting tortuosity was 1.6. The self diffusion coefficient of water at the same temperature (25 ºC) is 2.5 x 10^{-5} cm^2 s^{-1} [83, 84]. Hence, the diffusion of water in wood is slower than its self-diffusion, which is reasonable. For the sulfide ion, D_e is 5.73 x 10^{-5} cm^2 s^{-1}, which is nominally faster than the self diffusion coefficients of 1.731 x 10^{-5} cm^2 s^{-1} [9] for hydrosulfide or 2.6 x 10^{-5} cm^2 s^{-1} [97] for sulfide. Clearly, these unusual values for tortuosity and D_e indicate that there is more to the process than simple Fickian diffusion.

These anomalies can be reconciled if charge exclusion is considered. Cellulose and hemicellulose comprise the largest component of wood by weight. The surface of cellulose in contact with water is negatively charged [98, 99]. The negatively charged sulfide ion could be excluded from diffusing into these negatively charged zones. As a result the volume accessible to the sulfide ion would be lower than expected on the basis of pore volume alone. This is the case in the work presented here, as seen in Figure 4-8. Chip porosity is another measure of the same phenomenon. The porosity of sulfide should be lower than that for more neutral species, which would lead to a low apparent

value for the tortuosity, as observed in the Table 4-2 results. Charge exclusion is quite well known in chromatography [100, 101]. Anion exclusion has been reported in soils, membranes, and microbial polysaccharides [102-106].

The term "effective porosity" has been used to describe a system where charge effects occur. In uncharged media the tortuosity is a geometric representation of the pore morphology. In charged systems, however, the pathways for cations and anions are different depending on the charge of the pore system [102]. This changes the porosity value of the individual ions. In a charged system such as the one studied here, the effective diffusivity of a charged ion could be considerably greater than that in an uncharged system.

Exclusion effects should also apply to the hydroxide ion. In one study, the hydroxide concentration in the interior of cellulose was much lower than that in the bulk solution. This difference increased with increasing hydroxide concentration [107]. The effect originates from the negative charge on the cellulose. Charge repulsion is, of course, also the basis of fibers swelling in strongly alkaline solution [108]. However, the lower apparent tortuosity for the sulfide ion suggests that it is more prone to exclusion than is hydroxide.

It follows that if the volume of the wood chip accessible towards sulfide is low, then sulfide would diffuse more rapidly into the body of the chip than would hydroxide. If the diffusion coefficients of sulfide and hydroxide are similar, then both species would

diffuse into similar volumes of water in the chip. However, if only sulfide was excluded from certain regions in the chip, then it would have to diffuse to a greater extent into the body of the chip to access the same volume of water available to the hydroxide. As a result, it would move faster towards the core.

This is cleanly demonstrated in Figures 4.9 – 4.12 where a sweetgum chip was immersed in hot white liquor for a few minutes and then split in two along the *z* direction; *i.e.* the chip was opened like a book. The black regions indicate sulfur ingress while the red areas show hydroxide ingress.

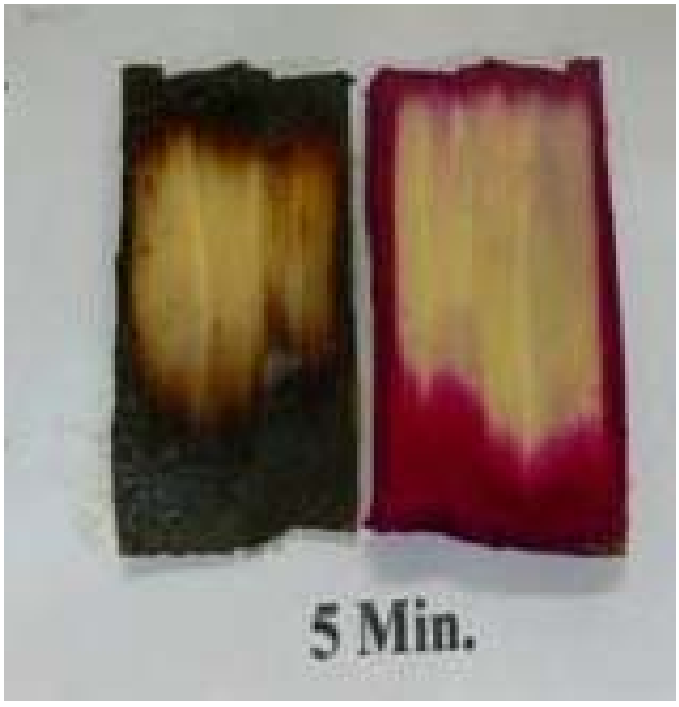

Figure 4-9 Sulfide and hydroxide diffusion into sweetgum at 5 minutes

Figure 4-10 Sulfide and hydroxide diffusion into sweetgum at 10 minutes

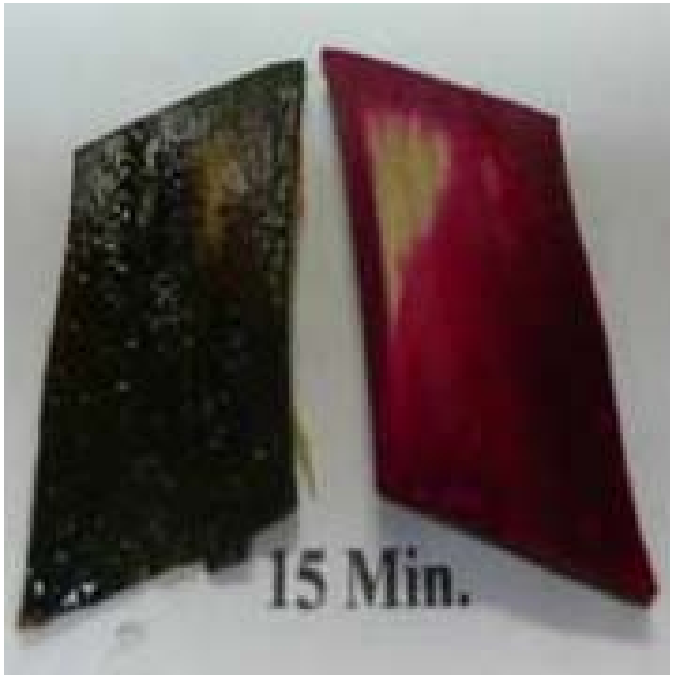

Figure 4-11 Sulfide and hydroxide diffusion into sweetgum at 15 minutes

Figure 4-12 Sulfide and hydroxide diffusion into sweetgum at 20 minutes

One half was sprayed with phenolphthalein to image the ingress of the hydroxide ion; the other was stained with silver nitrate to outline the presence of sulfide. Analogous results for pine are shown in Figures 4.13 – 4.16.

Figure 4-13 Sulfide and hydroxide diffusion into pine at 5 minutes

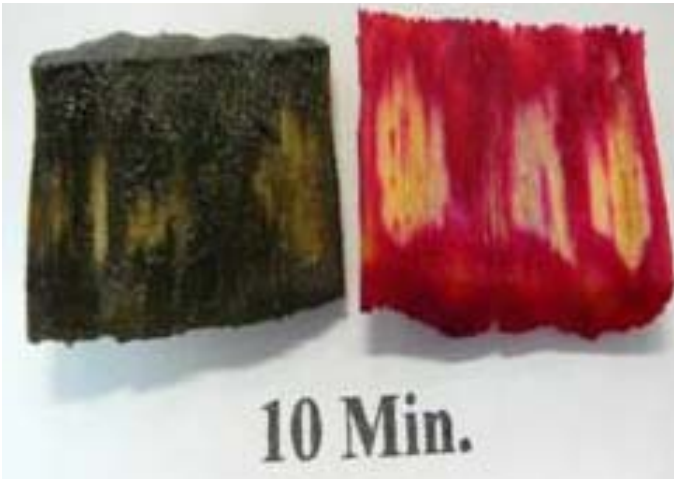

Figure 4-14 Sulfide and hydroxide diffusion into pine at 10 minutes

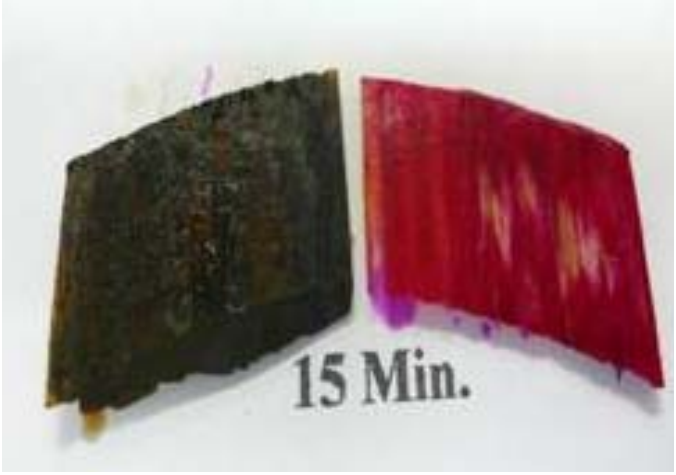

Figure 4-15 Sulfide and hydroxide diffusion into pine at 15 minutes

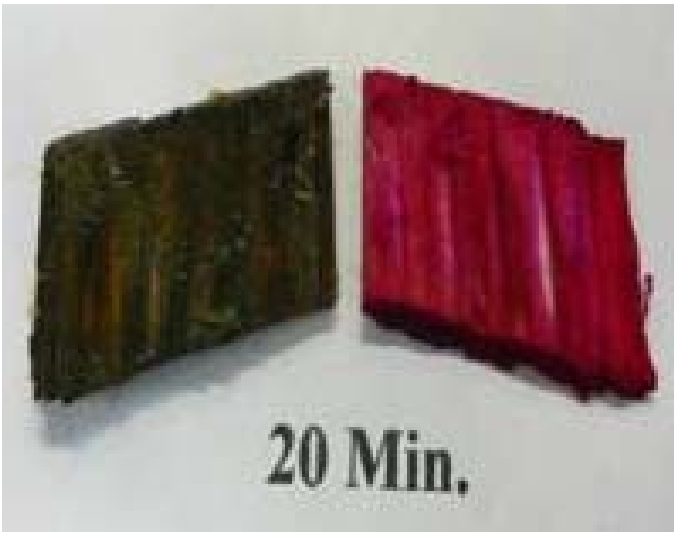

Figure 4-16 Sulfide and hydroxide diffusion into pine at 20 minutes

As a point of record Gustafson et al.[109] stained wood chips with phenolphthalein as was done here to study the penetration of cooking chemicals into woodchips. However, our use of dual indicators to simultaneously study the movement of sulfide appears to be new.

The illustrations in Figures 4.9 – 4.16 provide compelling evidence that the sulfide reaches the core of the chip well before hydroxide does. Some of the hydroxide will be consumed by wood acids as it enters the chip. However, this loss should not slow down the hydroxide diffusion front significantly. The phenolic groups [110], and glucuronic acid groups[111] add up to 0.00025 moles per gram of oven-dry wood. Even if they were all available to react (which is unlikely), they would consume only about 6% of the hydroxide diffused into the wood. Hence, the results in Figures 4.9 – 4.16 are consistent with the lower porosity of the wood towards sulfide ion.

The difference between hydroxide and sulfide porosity explains why it is important to have a high sulfide:hydroxide ratio during early pulping. It follows that a part of the chip will be exposed to principally hydroxide during early pulping because the sulfide will be occluded from these regions. Indeed, sections of wood will be exposed to much higher hydroxide:sulfide ratios than that present in the bulk liquor. Reducing this ratio will minimize the degree of carbohydrate degradation. It is well-known that a high sulfide/hydroxide ratio early in the cook leads to optimal pulping [112, 113]. Our results could offer an explanation as to why this is so. If only hydroxide is allowed into certain parts of the chip, then carbohydrate degradation will occur without appreciable delignification. Increasing the sulfide/hydroxide ratio will counter this effect by minimizing the concentration of hydroxide in the sulfur-occluded regions. Presumably these regions will open up to sulfur as delignification progresses and the composition of the chip changes.

The above discussion relates to time periods of a few seconds where the diffusion is assumed to be reversible. However, sulfide is known to irreversibly bind to wood components [114]. In order to demonstrate that irreversible binding does not occur in our time frame, the loss of sulfide from white liquor was followed for prolonged periods. Results for both short and long time scales are shown in Figure 4-17 and Figure 4-18.

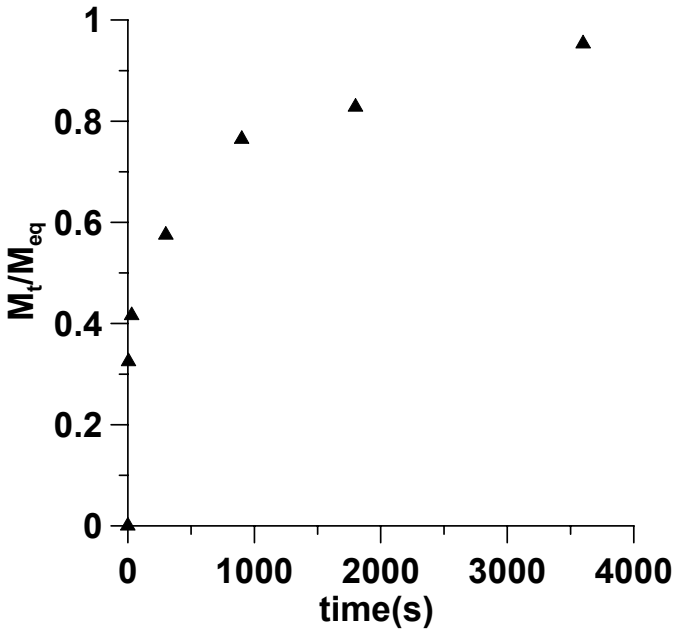

Figure 4-17 Diffusion of sulfide into pine particles

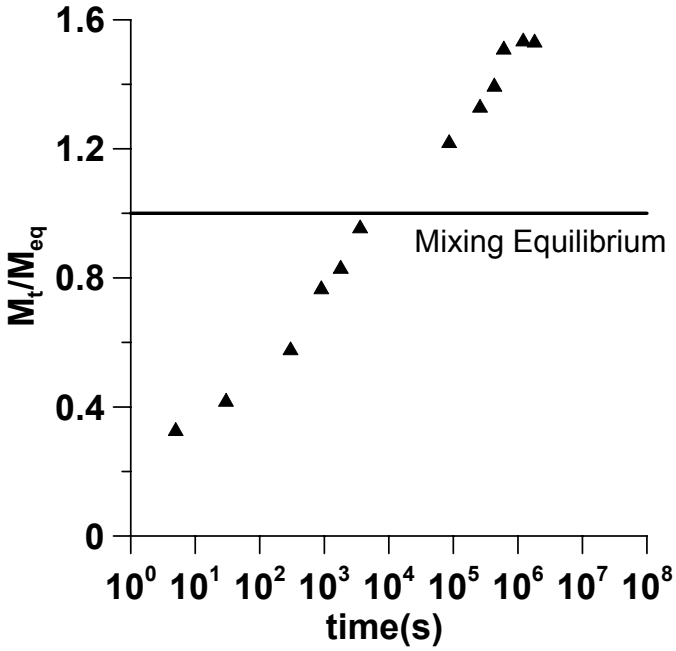

Figure 4-18 Diffusion of sulfide into pine particles at long times

The sulfide content of the wood increases beyond the equilibrium value over the longer time frame, which is consistent with irreversible binding. However, this occurs too slowly to affect the steady-state situation reached in the more rapid experiments from which the tortuosity values were derived.

In summary, this work has shown that when a chip is initially exposed to white liquor, the effective porosity of the chip towards sulfide ion is lower that that towards hydroxide, and the sulfide is able to enter the interior of the wood much faster than does hydroxide. The proposed reason is that the sulfide is excluded from highly negatively charged areas in the wood because of charge exclusion. As a result, the hydroxide:sulfide ratio could be much higher in the excluded regions than in the bulk liquor. Pretreatment with green liquor and other high sulfidity/low alkalinity media will help compensate for this

situation by allowing the sulfide more time to diffuse into regions in the wood where its diffusivity is low.

4.3 Results from Fines Pulping

This thesis reports the results of how water and sulfide diffuse into uniform size wood particles. Since the diffusion of chemicals is important in kraft pulping, the same size particles used in the diffusion experiments were used for kraft cooking. The tritiated water results suggest that diffusion is hindered for smaller particles and experiments were done to determine if this extended into pulping.

A previous study showed that if hardwood fines are added to a cook with conventionally sized chips, the amount of fiber fines increases[82]. Since this did not occur in softwood cooks, it was possible that the fines were being consumed during the cook. Kraft cooks were done on pine chips containing 20 percent fines. As shown in Figure 4-19, there is no correlation between the H-factor and amount of fiber fines produced for these conditions.

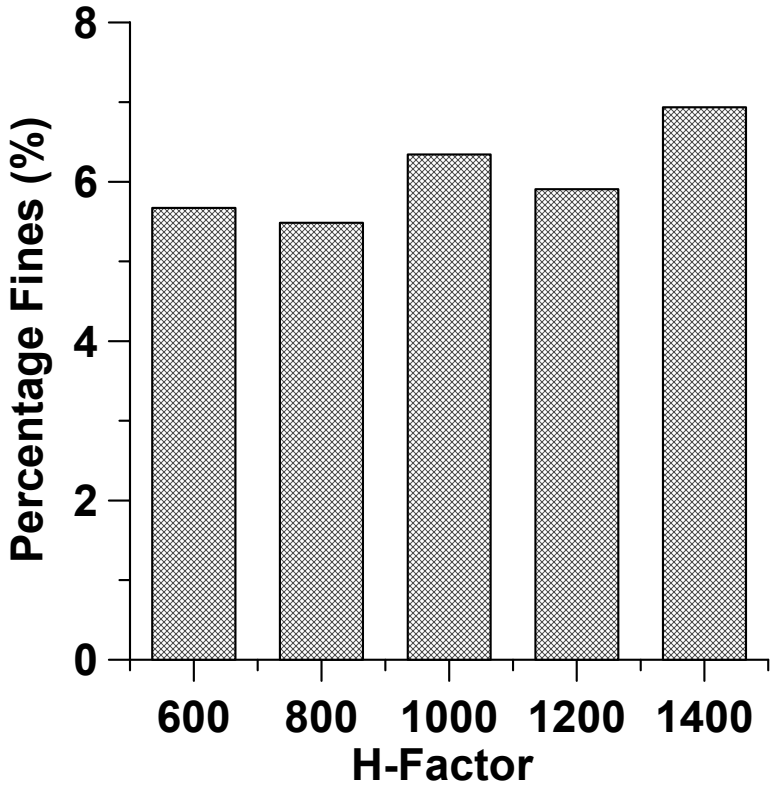

Figure 4-19 Fiber fines percentage of pulp versus extent of cooking (H-factor)

The amount of fiber fines did not decrease throughout the cook. It seemed that the pine wood fines did not have any effect on the amount of fiber fines produced. When a similar study was done with hardwood, there was no correlation between extent of cooking and fiber fines produced. More importantly, the control cook that had no wood fines added had the same amount of fiber fines produced as the cook with 20 percent fines added in. This did not agree with the previous study. The difference between the experiments was that the fines for the present experiments were generated on a Wiley mill and screened through a 3 mm hole screen.

The fines produced in the Wiley mill and those sent from the mill were different. Both fines fell through a 3mm hole screen but gave different amount of fiber fines produced

when pulped. A more extensive size classification was done on the different fines used in this experiment. Tyler sieves mounted to an automatic shaker were used to classify the 3 mm screened particles. Table 4-3 shows the results of the fractionation.

Table 4-3 Size classification of fines used in pulping experiments

Sieve size range (mm)	Weight (%)		
	Sweetgum - Wiley fines	Mix Hardwood - Mill Fines	Pine - Mill Fines
>2.00	5.6%	6.4%	53.5%
1.70 - 2.00	13.0%	9.0%	12.2%
1.40 - 1.70	22.8%	18.0%	13.2%
1.00 - 1.40	34.4%	23.9%	15.1%
1.000 - 0.850	9.9%	3.3%	6.1%
0.850 - 0.600	11.5%	17.1%	--
0.600 - 0.425	2.7%	15.5%	--
0.425 - 0.180	0.0%	6.7%	--
<0.180	0.0%	0.1%	--

It is clear that most of the pine fines contain mostly large wood particles. This could be the reason why no additional fiber fines are created when the wood fines are added. The hardwood fines contain smaller particles, but there is a difference between the two. Figure 4-20 shows the difference between the hardwood fines from the mill and those generated on a Wiley mill.

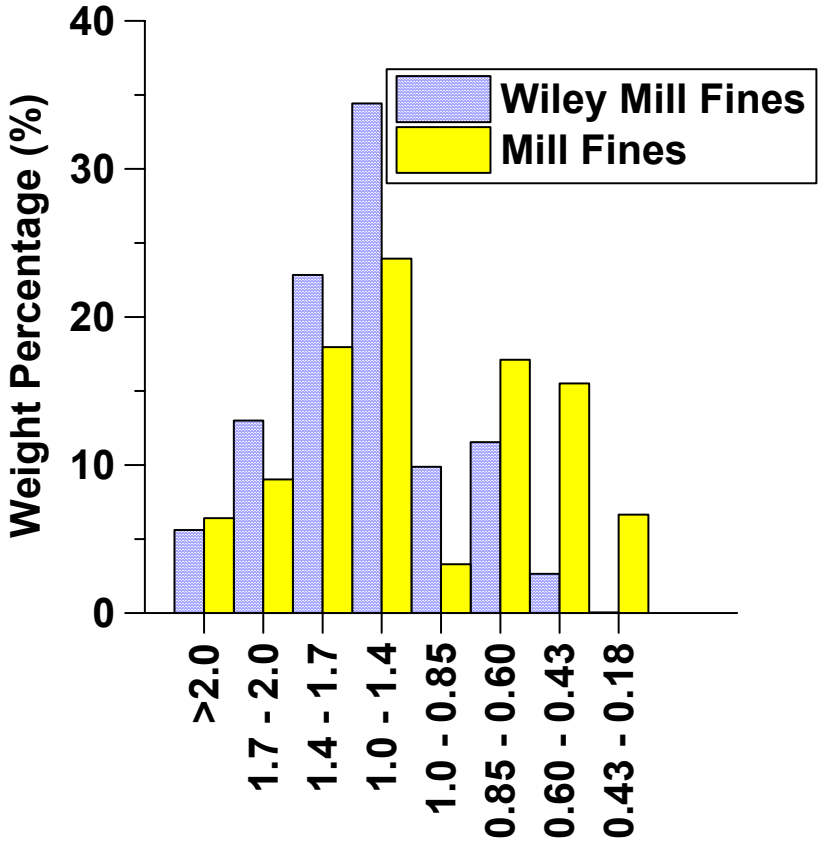

Figure 4-20 Size classification of fines sent from mill and fines produced on Wiley mill

Although both fines fell through a 3mm hole, the mill fines contain smaller particles than the Wiley mill fines. The data clearly show that even though something is classified as wood fines by passing through a 3mm hole screen, there still can be major differences in particle size composition.

The next set of experiments was done by pulping only the wood particles from a particular size fraction. Sweetgum chips were broken up with a Wiley mill and the subsequent particles were fractionated with Tyler sieves. The cooking conditions were the same as before, except that the liquor to wood ratio was increased to 6:1. Figure 4-21 shows the fiber length of the different size fractions.

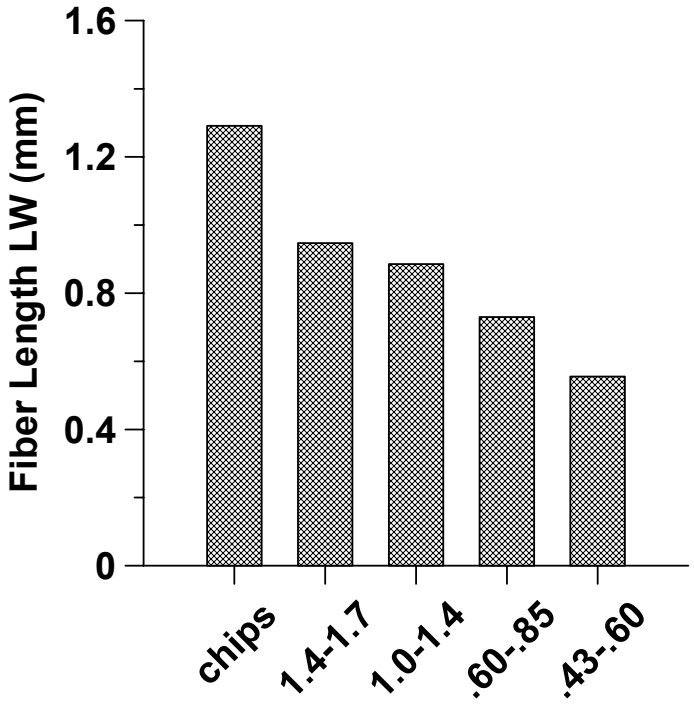

Figure 4-21 Length-weighted fiber length of pulp made from sweetgum particles

The fiber length results are as expected. Smaller particles will give shorter fibers. Figure 4-22 shows the fiber fines generated from sweetgum wood particles.

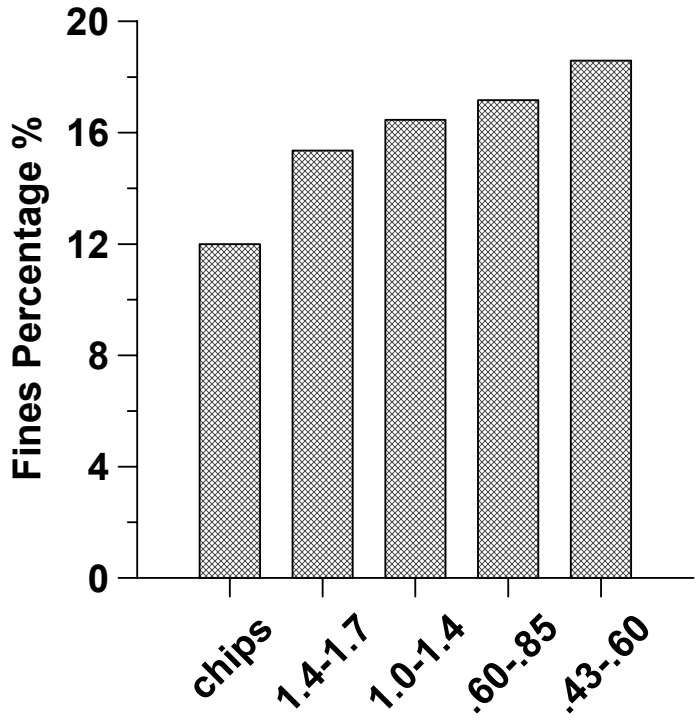

Figure 4-22 Fiber fines percentage of pulp made from sweetgum particles

As the particle size decreases, more fiber fines are generated in the resulting pulp. The increase is dramatic, the smallest particle size gives almost 20 percent fiber fines.

Pine sawdust pulping was completed next. Table 4-4 shows the results for the pine sawdust.

Table 4-4 Summary of results for kraft cooking of pine particles

Size (mm)	H factor	Kappa #	Fines weight%	Fiber length (mm)
.43-.60	1400	82.6	11.2%	0.81
.60-.85	1400	96.1	8.6%	1.22
.85-1.0	1400	85.5	5.7%	1.39
1.0-1.4	1400	89.1	4.8%	1.53
1.4-1.7	1400	79.5	4.8%	1.66
Chips	1400	32.4	6.0%	2.78

As expected, the fiber length decreased as the particle size decreased. Figure 4-23 shows graphically the fiber length for the different particle sizes.

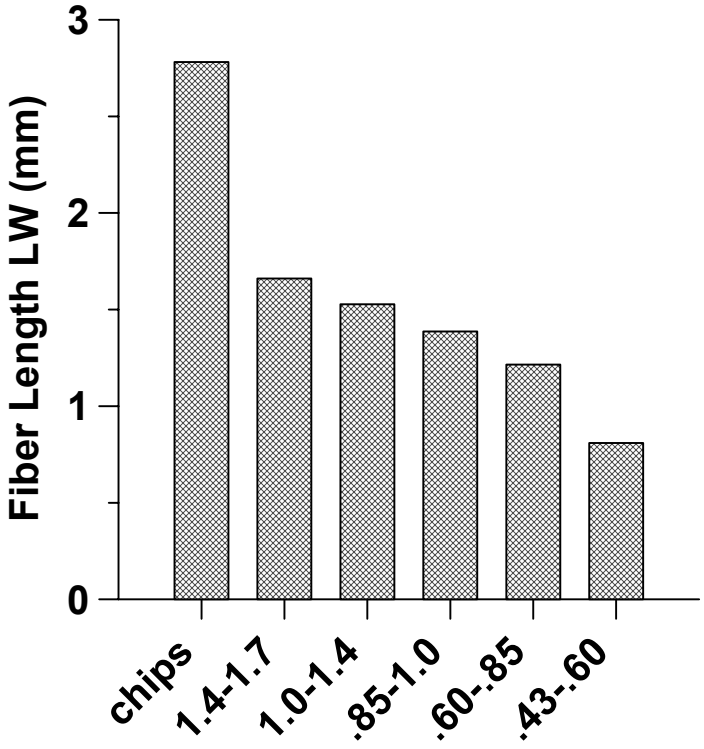

Figure 4-23 Length-weighted fiber length of pulp made from pine particles

The small particles give fibers that are similar to hardwood fiber lengths. Figure 4-24 shows the amount of fiber fines produced for each size fraction.

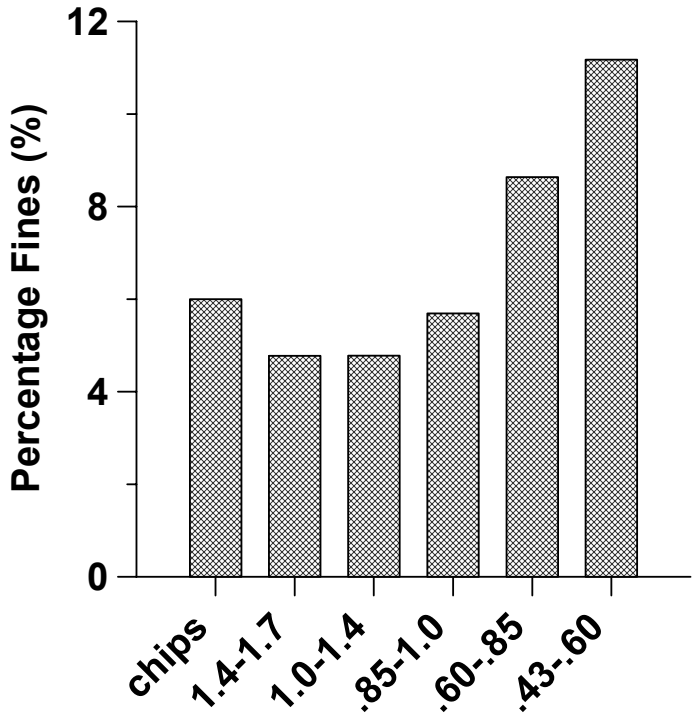

Figure 4-24 Fiber fines percentage of pulp made from pine particles

Once the particle size gets below the 0.85 mm threshold, the amount of fiber fines start to increase drastically. Typical pine chips give about 5 percent fiber fines but with the smallest particles it increased to 11 percent. In an industrial pulping operation, the wood particles that are classified as fines might be different in size depending on where the wood particles came from. This could lead to variability in finished pulp that could potentially cause problems on the paper machine.

Another unexpected event occurred while pulping the pine sawdust. The sawdust pulp had a high kappa number compared to the pulped wood chips. The kappa number test was repeated and the same high kappa numbers were found. The only difference in cooking conditions between sawdust pulping and chip pulping was the liquor to wood ratio and hence the concentration of the active pulping chemicals in the digester. Various

cooking conditions were applied to both chips and wood particles to determine why the pine particles had a higher kappa number. Table 4-5 shows the cooking conditions and the results for the pine cooks.

Table 4-5 Pulping conditions and results of pine particles and pine chips

Run	Size	White Liquor		L:W ratio	H-factor	Kappa #
		%AA on wood	AA g/L as Na_2O			
1	chips	18	50	4:1	1400	31.6
2	sawdust .425 - .600	18	31	6:1	1400	78.7
3	sawdust .600 - .850	18	31	6:1	1400	91.7
4	sawdust .850 - 1.0	18	31	6:1	1400	81.4
5	sawdust 1.0 - 1.4	18	31	6:1	1400	85.4
6	sawdust 1.4 - 1.7	18	31	6:1	1400	75.0
7	sawdust 1.0 - 1.4	27	50	6:1	1400	28.5
8	chips	27	50	6:1	1400	29.5
9	chips	18	31	6:1	1400	50.6
10	sawdust 1.4 - 1.7	18	31	6:1	1400	73.0

When the pine chips were cooked under the same conditions as the sawdust, the pulp gave a higher kappa number (50.6) than normal (30). However, the sawdust pulp gave kappa numbers around 80. The sawdust was then cooked with a higher concentration of alkali and the kappa number was back down to 30. This implies that pine sawdust pulping requires more alkali to pulp to the same kappa number compared to normal chip pulping. This increased alkali requirement has been reported elsewhere[115]. One way to combat the need for increased alkali is to use anthraquinone in the cooking formula[116].

Pulping sweetgum sawdust did not require any additional alkali. The sweetgum sawdust had a higher liquor to wood ratio and hence had a lower concentration of alkali in the liquor, but still pulped to the same low kappa number of the chip pulp. As mentioned

earlier, hardwood lignin is easier to pulp than softwood lignin, and southern pine has a higher percentage of lignin than sweetgum[85, 87]. It may be that the sweetgum sawdust requires more alkali to pulp but our experiments may have had excess alkali for the cooks.

In Kraft cooking of wood fines or sawdust, the product quality is ultimately determined by the size of the particles. The experiments have shown that classifying fines as particles that pass through a 3 mm hole screen will give fiber variability depending on the wood species and how it was produced.

CHAPTER 5

CONCLUSIONS

In this thesis, it was shown that Fickian diffusion describes how water will diffuse into the water filled pores of wood. Modeling of the transport of tritiated water into the wood particles was successful using a 1-dimensional cylindrical model. Aspen and pine particles used in the experiments are representative of the two major classifications of trees, hardwood and softwood respectively. The wood particles were fractionated and many different sizes were used. The amount of tritiated water that diffused into the wood particles was same as the calculated amount it the tritiated water had only mixed with the amount of water in the wood. There were no regions of the wood where the tritiated water could not diffuse into.

The diffusion into and out of the particles is nearly identical, demonstrating that diffusion of water into saturated wood particles is completely reversible. There was no hysteresis for the saturated wood as is common for water adsorption into unsaturated wood. Therefore, all the regions in fully saturated wood are equally accessible to the diffusing water molecules. Water that is highly bound to the wood structure readily exchanges with the loosely bound bulk water.

It was shown that as particles decreased in size the tortuosity increased. This effect was more pronounced for the aspen particles. This effect has been observed elsewhere and may be due to porosity fluctuations or from pore closure from excessive processing of the

small particles. Aspen had higher tortuosity values than pine, most likely resulting from aspen's shorter fiber lengths.

Similar diffusion experiments with sulfide yielded much different results. As sulfide diffused into pine, it would level off at a point that was much lower than if the sulfide completely mixed with the wood moisture. There were clearly areas in the wood where sulfide could not diffuse into at that time frame. The calculated diffusion coefficients for sulfide were higher than the self-diffusion coefficient. This was yielding tortuosity values that were less than one which physically are impossible.

An explanation of these results may be charge exclusion of the sulfide ion by the negatively charged surfaces of wood. The negatively charged sulfide ion could be excluded from diffusing into these negatively charged zones. As a result the volume accessible to the sulfide ion would be lower than expected on the basis of pore volume alone. The porosity towards sulfide should be lower than that for more neutral species, which would lead to a low apparent value for the tortuosity. Therefore, a diffusing species into wood is not only influenced by its diffusion coefficient in water but also the interaction with surfaces of wood. This will lead to molecules that have different effective porosities in wood depending on the specific interaction with the negative surfaces of wood. Charge exclusion occurs in other media such as soils and membranes.

The concept of sulfide diffusing rapidly into wood was verified when chips were soaked in white liquor, split open and sprayed with indicator solution. The sulfide was clearly

transporting further into the chips than hydroxide. If sulfide is excluded from regions in wood that hydroxide is not, it will continue to diffuse into regions that are available to it. This will give the appearance that the sulfide is diffusing faster into the center of the chip when it is just diffusing into the areas where it is not excluded.

In kraft pulping it is has been shown that pre-treatment of wood chips with high sulfidity solutions will lead to optimal pulping. The results of this work may offer an explanation of this pretreatment and also why it is important to have a high sulfide:hydroxide ratio at the beginning of a cook. Hydroxide will diffuse into regions where sulfide is occluded from and may participate in cellulose degradation reactions. These regions may have a higher hydroxide:sulfide ratios than found in the bulk liquor. Allowing greater time of contact with sulfide might allow it to diffuse into occluded regions. In addition, polysulfide treatment may have a huge advantage over negatively charged sulfide ions due to polysulfide's neutrality and thus ability to diffuse into regions that may be blocked off to negatively charged sulfide ions.

Kraft pulping of wood fines and sawdust is different from pulping normal wood chips. Besides producing pulp with shorter fiber lengths, very small sawdust will produce a higher degree of pulp that is classified as fiber fines which may have an effect on downstream operations. Pine sawdust pulping requires more alkali than cooking of pine chips. No such increase chemical usage was needed for sweetgum sawdust cooking.

REFERENCES

1. Brown, R., *A brief account of microscopical observations made in the months of June, July and August, 1827, on the particles contained in the pollen of plants; and on the general existence of active molecules in organic and inorganic bodies.* Philosophical Magazine, 1828. **4**: p. 161-173.

2. Fick, A., Philosophical Magazine, 1855. **10**: p. 30.

3. Einstein, A., *Über die von der molekularkinetischen Theorie der Wärme geforderte Bewegung von in ruhenden Flüssigkeiten suspendierten Teilchen.* Annals of Physics, 1905. **17**: p. 549.

4. Sherwood, T.K., R.L. Pigford, and C.R. Wilke, *Mass Transfer*. 1975, New York: McGraw-Hill.

5. Fuller, E.N., P.D. Schettler, and J.C. Giddings, Industrial & Engineering Chemistry, 1966. **58**(19).

6. Hirschfelder, J.O., R.B. Bird, and E.L. Spotz, Chemical Reviews, 1949. **44**(205).

7. Hines, A.L. and R.N. Maddox, *Mass Transfer*. 1985, Upper Saddle River: Prentice-Hall.

8. Wilke, C.R. and P. Chang, *Correlation of Diffusion Coefficients in Dilute Solutions.* AIChE Journal, 1955. **1**: p. 264-270.

9. Perry, R.H. and D.W. Green, *Perry's Chemical Engineers' Handbook*. 7th ed. 1997: McGraw-Hill. 2581.

10. Vignes, A., *Diffusion in Binary Solutions.* Industrial and Engineering Chemistry Fundamentals, 1966. **5**(2): p. 189-199.

11. Leffler, J. and H.T. Cullinan, *Variation of Liquid Diffusion Coefficients with Composition - Binary Systems.* Industrial and Engineering Chemistry Fundamentals, 1970. **9**(1): p. 84-88.

12. Knudsen, M., *Die Gesetze der Molekularstromung und der inneren Reibungsstromung der Gase durch Rohren (The Laws of Molecular Flow and of Inner Friction Flow of Gases Through Tubes).* Annalen der Physik, 1909. **28**: p. 75-130.

13. Hakkila, P., *Forest Resources and Sustainable Management*. Papermaking Science and Technology. 2000, Helsinki: Fapet Oy.

14. Smook, G.A., *Characteristics of Wood and Wood Pulp Fibers*, in *Handbook for Pulp and Paper Technologists*. 1990, Angus Wilde Publications: Vancouver.

15. Hale, J.D., *Structural and Physical Properties of Pulpwood*, in *The Pulping of Wood*, R.G. MacDonald, Editor. 1969, McGraw-Hill: New York. p. 1-32.

16. Alén, R., *Forest Products Chemistry*. Papermaking Science and Technology. 2000, Helsinki: Fapet Oy.

17. Thomas, M., G. Malcolm, and E.W. Malcolm, *Alkaline Pulping*. Pulp and Paper Manufacture. Vol. 5. 1989: Tappi Press.

18. Sarkanen, K.V. and C.H. Ludwig, *Lignins: occurrence, formation, structure and reactions*. 1971, New York: Wiley. 916.

19. Karhunen, P., et al., *Dibenzodioxocins; A Novel Type of Linkage in Softwood Lignins.* Tetrahedron Letters, 1995. **36**(1): p. 167-170.

20. Adler, E., *Lignin - Past, Present and Future.* Wood Science and Technology, 1977. **11**(3): p. 169-218.

21. Panshin, A.J. and C. de Zeeuw, *Textbook of Wood Technology*. 1980, New York: McGraw-Hill.

22. Stamm, A.J., *Wood and Cellulose Science*. 1964, New York: The Roland Press Company. 549.

23. Timmell, T.E., *Recent progress in the chemistry and topochemistry of compression wood.* Wood Science and Technology, 1981. **16**: p. 83-122.

24. Kouali, M.E. and J.M. Vergnaud, *Modeling the process of absorption and desorption of water above and below the fiber saturation point.* Wood Science and Technology, 1991. **25**: p. 327-339.

25. Tiemann, H.D., *Effect of Moisture upon the Strength and Stiffness of Wood.* US Department of Agriculture Bull, 1906. **70**: p. 144.

26. Nakamura, K., T. Hatakeyma, and H. Hatakeyma, *Studies on Bound Water of Cellulose by Differential Scanning Calorimetry.* Journal of Textile Institute, 1981. **72**(9): p. 607-613.

27. Nelson, R.A., *The Determination of Moisture Transitions in Cellulosic Materials Using Differential Scanning Calorimetry.* Journal of Applied Polymer Science, 1977. **21**: p. 645-654.

28. Karenlampi, P.P., P. Tynjala, and P. Strom, *Phase Transformations of Wood Cell Wall Water.* Journal of Wood Science, 2005. **51**: p. 118-123.

29. Hartley, I.D., F.A. Kamke, and H. Peemoeller, *Cluster Theory for Water Sorption in Wood.* Wood Science and Technology, 1992. **26**: p. 83-99.

30. Lentz, B.R., A.T. Haglar, and H.A. Scheraga, *Structure of Liquid Water. II. Improved Statistical Thermodynamic Treatment and Implications of a Cluster Model.* Journal of Physical Chemistry, 1974. **78**: p. 1531-1550.

31. Goring, D.A.I., *The Effect of Cellulose on the Structure of Water: View 1*, in *Fibre Water Interactions in Paper-making*. 1978, The British Paper and Board Industry Federation: London.

32. Caulfield, D.F., *The Effect of Cellulose on the Structure of Water: View 2*, in *Fibre Water Interactions in Paper-making*. 1978, The British Paper and Board Industry Federation: London.

33. Polyani, M., Verhandlungen der Deutschen Physika- lischen Gesellschaft, 1924. **16**: p. 1012.

34. Morrison, J.L. and M.A. Dzieciuch, Canandian Journal of Chemistry, 1959. **37**: p. 1379.

35. Collins, G., Journal of Textile Institute, 1930. **21**: p. 311.

36. Kleppe, P.J., *Kraft Pulping.* Tappi Journal, 1970. **53**(1): p. 35-47.

37. Biermann, C.J., *Essentials of Pulping and Papermaking*. 1993, San Diego: Academic Press Inc. 471.

38. Rydholm, S., *Pulping Processes*. 1965, New York: Wiley.

39. Svenson, S., *Method of and an Apparatus to Charge Cellulose Digesters or the Like*. 1936: United States.

40. Gullichsen, J. and H. Sundqvist. *On the Importance of Impregnation and Chip Dimensions on the Homogeneity of Kraft Pulping*. in *Pulping Conference*. 1995. Chicago.

41. Gustafsson, R.R., et al. *The role of penetration and diffusion in pulping non-uniformity of softwood chips*. in *Pulping Conference*. 1988. New Orleans.

42. Malkov, S., P. Tikka, and J. Gullichsen, *Towards Complete Impregnation of Wood Chips with Aqueous Solutions. Part 1. A Retrospective and Critical Evaluation of the Penetration Process.* Paperi ja Puu, 2003. **85**(8): p. 460-466.

43. Stamm, A.J., *Diffusion and Penetration Mechanism of Liquids into Wood.* Pulp and Paper Magazine of Canada, 1953. **54**(2): p. 54-63.

44. Mckee, W.F., *The Effect of Wood Handling and Chip Preparation on Sulphite Pulp Yield and Quality.* Pulp and Paper Magazine of Canada, 1952. **53**(3): p. 237-240.

45. Jimenez, G., et al. *Experimental and Theoretical Studies to Improve Pulp Uniformity*. in *TAPPI Pulping Conference Proceedings*. 1990. Toronto.

46. Maass, O., *The Problem of Penetration.* Pulp & Paper Magazine of Canada, 1953. **54**(8): p. 98-103.

47. Paranyi, N.I. and W. Rabinovitch, *Determination of Penetration Rate of Liquid Media into Wood Using a Quartz Spiral Balance.* Pulp and Paper Magazine of Canada, 1995. **56**(3): p. 164-170.

48. Hartler, N. and W. Onisko, *The interdependence of chip thickness, cooking temperature and screenings in kraft cooking of pine.* Svensk Papperstidning, 1962. **65**(22): p. 905-910.

49. Gullichsen, J., *Chemical Engineering Principles of Fiber Line Operations*, in *Chemical Pulping*. 2000, Fapet Oy: Helsinki.

50. Lonnberg, B., L. Robertson, and K. Saari. *Chemical Diffusion in Wood*. in *AICHE Forest Products Symposium*. 1992.

51. de Montigny, R. and O. Maass, *Investigation of Physico-chemical Factors which Influence Sulphite Cooking*, in *Forest Service Bulletin 87*. 1935: Canada.

52. Meyer, R.W., *Effect of Enzyme Treatment on Bordered-Pit Ultrastructure, Permeability, and Toughness of the Sapwood of Three Western Conifers.* Wood Science, 1974. **6**(3): p. 220-230.

53. Jacobs-Young, C.J., R.A. Venditti, and W.J. Thomas, *Effect of enzymatic pretreatment on the diffusion of sodium hydroxide in wood.* Tappi Journal, 1998. **81**(1): p. 260-266.

54. Fischer, K., et al., *Reduction of resin content in wood chips during experimental biological pulping processes.* Holzforschung, 1994. **48**(4): p. 285-290.

55. Skaar, C. and J.F. Siau, *Thermal Diffusion of Bound Water in Wood.* Wood Science and Technology, 1981. **15**: p. 105-112.

56. Siau, J.F., *Transport Processes in Wood*. Springer Series in Wood Science, ed. T.E. Timmell. Vol. 2. 1984, Syracuse: Springer-Verlag. 225.

57. Nakano, T., *Non-Steady State Water Adsorption of Wood.* Wood Science and Technology, 1994. **28**: p. 359-363.

58. Robertson, L. and B. Lonnberg, *Diffusion in Wood.* Paperi ju Puu, 1991. **73**(6): p. 532-535.

59. Talton, J., *The Diffusion of Sodium Hydroxide in Wood at High pH as a function of Temperature and Degree of Pulping*. 1986, North Carolina State University. p. 45.

60. Gustafson, R., C. Sleicher, and W. Mckean, *Theoretical Model of the Kraft Pulping Process.* Industrial Engineering Chemical Process Design & Development, 1983. **22**(1): p. 87-96.

61. Kohne, J.M., H.H. Gerke, and S. Kohne, *Effective Diffusion Coefficients of Soil Aggregates with Surface Skins.* Soil Science Society of America Journal, 2002. **66**(September-October): p. 1430-1438.

62. Nitta, K., M. Natsuisaka, and A. Tanioka, *Measurements of Self-Diffusion Coefficients of Water in Porous Membranes by PFG-NMR.* Desalination, 1999. **123**: p. 9-14.

63. Hutchison, J.M., et al., *Chromate transport and retention in variably saturated soil columns.* Vadose zone Journal, 2003. **2**: p. 702-714.

64. Kendall, C. and J.J. McDonnell, *Isotope Tracers in Catchment Hydrology*. 1998, Amsterdam: Elselvier. 839.

65. Livingston, H.D. and P.P. Povinec, *A millennium perspective on the contribution of global fallout radionuclides to ocean science.* Health Physics, 2002. **82**: p. 656-668.

66. Carey, F.A., *Organic Chemistry*. 4th ed. 2000: McGraw-Hill. 1108.

67. Bothner, A.A. and C. Sun, *Acid and Base Catalyzed Hydrogen-Deuterium Exchange between Deuterium Oxide and Simple Ketones.* Journal of Organic Chemistry, 1967. **32**: p. 492-493.

68. Rappe, C. and W.H. Sachs, *Enolization of ketones. IV. Rate and orientation of base-catalyzed deuteration of some methyl ketones.* Journal of Organic Chemistry, 1967. **32**(12): p. 4127-4128.

69. Biemann, K., *Mass Spectrometry: Organic Chemical Applications.* McGraw-Hill series in advanced chemistry. 1962, New York: McGraw-Hill. 370.

70. Beckman, *LS 5801 Liquid Scintillation Systems Operating Manual*. 1985, Irvine: Beckman Instruments.

71. Horrocks, D.L., *Effects of Impurity and Color quenching Upon the Liquid Scintillation Pulse Height Distributions*, in *Liquid Scintillation Counting: Recent Applications and Development*, C. Peng, D. Horrocks, and E. Alpen, Editors. 1980, Academic Press.

72. Rasband, W.S., *ImageJ*. 1997-2004, National Institutes of Health: Bethesda, Maryland.

73. Rao, P.S.C., R.E. Jessup, and T.M. Addiscott, *Experimental and Theoretical Aspects of Solute Diffusion in Spherical and Nonspherical Aggregates.* Soil Science, 1982. **133**(8): p. 342-349.

74. Crank, J., *The Mathematics of Diffusion*. 2nd ed. 1975, Oxford: Clarendon Press. 414.

75. Dean, W.M., *Solution Methods for Condcution and Diffusion Problems*, in *Analysis of Transport Phenomena*. 1998, Oxford University Press: New York. p. 132-194.

76. Jahnke, E. and F. Emde, *Tables of Functions with Formulae and Curves*. 1945, New York: Dover Publications.

77. Van Der Kamp, G., D.R. Stempvoort, and L.I. Wassenaar, *The Radial Diffusion Method 1. Using Intact Cores to Determine Isotopic Composition, Chemistry, and Effective Porosities for Groundwater in Aquitards.* Water Resources Research, 1996. **32**(6): p. 1815-1822.

78. TAPPI, *Analysis of Soda and Sulfate White and Green Liquors TAPPI Test Method T 624 cm – 00*. 2000.

79. TAPPI, *Kappa number of pulp TAPPI Test Method T 236 om – 99.* 1999.

80. TAPPI, *Solids content of black liquor TAPPI Test Method T 650 om – 05.* 2005.

81. TAPPI, *Fines fraction by weight of paper stock by wet screening TAPPI Test Method T 261 cm – 00.* 2000.

82. Courchene, C., et al., *Improving Fiber Quality for Tissue-Making*. 2005, Georgia Institute of Technology. p. 13.

83. Pruppacher, H.R., *Self-Diffusion Coefficient of Supercooled Water.* The Journal of Chemical Physics, 1972. **56**(1): p. 101-107.

84. Mahoney, M.W. and W.L. Jorgensen, *Diffusion Constant of TEP5P model of liquid water.* Journal of Chemical Physics, 2001. **114**(1): p. 363-366.

85. Isenberg, I.H., *Pulpwoods of the United States and Canada - Conifers*. Third ed. Vol. 1. 1980, Appleton: The Institute of Paper Chemistry. 219.

86. Price, W.S., H. Ide, and Y. Arata, *Self-Diffusion of Supercooled Water to 238 K Using PGSE NMR Diffusion Measurements.* Journal of Physical Chemistry A, 1999. **103**: p. 448-450.

87. Isenberg, I.H., *Pulpwoods of the United States and Canada - Hardwoods*. Third ed. Vol. 2. 1981, Appleton: The Institute of Paper Chemistry. 168.

88. Evans, J.R., et al., *Kinetics of Cadmium Uptake by Chitosan-based Crab Shells.* Water Research, 2002. **36**: p. 3219-3226.

89. Adanez, J., P. Gayan, and F. Garcia-Labiano, *Comparison of Mechanistic Models for the Sulfation Reaction in a Broad Range of Particle Sizes of Sorbents.* Industrial & Engineering Chemistry Research, 1996. **35**(7): p. 2190-2197.

90. Shackelford, C.D. and D.E. Daniel, *Diffusion in Saturated Soil. I: Background.* Journal of Geotechnical Engineering, 1991. **117**(3): p. 467-483.

91. Gillham, R.W., et al., *Diffusion of nonreactive and reactive solutes through fine grained barrier materials.* Canadian Geotech Journal, 1984. **21**(3): p. 541-550.

92. Van Rees, K.C.J., et al., *Evaluation of Laboratory Techniques for Measuring Diffusion Coefficients in Sediments.* Environmental Science Technology, 1991. **25**(9): p. 1605-1611.

93. Rao, P.S.C., et al., *Experimental and Mathematical Description of Nonadsorbed Solute Transfer by Diffusion in Sperical Aggregates.* Soil Science Society of America Journal, 1980. **44**: p. 684-688.

94. Stamm, A.J., *Bound-Water Diffusion into Wood in the Fiber Direction.* Forest Products Journal, 1959. **9**: p. 27-32.

95. Pang, S. and A.N. Haslett, *The Application of Mathematical Models to the Commercial High-Temperature Drying of Softwood Lumber.* Drying Technology, 1995. **13**(8&9): p. 1635-1674.

96. Martin, M. and L. Canteri, *A Non Destructive Method for Quantifying the Wood Drying Quality Used to Determine the Intra and Inter Species Variability.* Drying Technology, 1997. **15**(5): p. 1293-1325.

97. Shimizu, K. and R.A. Osteryoung, *Determination of Diffusion Coefficients of Anions at a Rotating Silver Disk Electrode.* Analytical Chemistry, 1981. **53**: p. 2350-2351.

98. Poots, V.J.P. and G. McKay, *The Specific Surfaces of Peat and Wood.* Journal of Applied Polymer Science, 1979. **23**: p. 1117-1129.

99. Vickerstaff, T., *The Physical Chemistry of Dyeing*. 1954, London: Oliver and Boyd. 192.

100. Johnson, E.L. and R. Stevenson, *Basic Liquid Chromatography*. 1978, Palo Alto: Varian Associates, Inc.

101. Skoog, D.A., F.J. Holler, and T.A. Nieman, *Principles of Instrumental Analysis*. 5th ed. 1998, Orlando: Harcourt Brace & Company. 849.

102. Smith, D., et al., *Theoretical Analysis of Anion Exclusion and Diffusive Transport Through Platy – Clay Soils.* Transport in Porous Media, 2004. **57**: p. 251-277.

103. Gvirtzman, H. and M. Magaritz, *Water and Anion Transport in the Unsaturated Zone Traced by Environmental Tritium*, in *Inorganic Contaminants in the Vadose Zone*. 1989. p. 190-198.

104. Gvirtzman, H. and S.M. Gorelick, *Dispersion and Advection in Unsaturated Porous Media Enhanced by Anion Exclusion.* Nature, 1991. **352**: p. 793-795.

105. Hart, T.D., J.M. Lynch, and A.H.L. Chamberlain, *Anion Exclusion in Mecrobial and Soil Polysaccharides.* Biology and Fertility of Soils, 2001. **34**: p. 201-209.

106. Schoen, R., J.P. Gaudet, and T. Bariac, *Preferential Flow and Solute Transport in a Large Lysimeter, under Controlled Boundary Conditions.* Journal of Hydrology, 1999. **215**: p. 70-81.

107. Motomura, H., S. Bae, and Z. Morita, *Dissociation of Hydroxyl Groups of Cellulose at Low Ionic Strengths.* Dyes and Pigments, 1998. **39**(4): p. 243-258.

108. Kazi, K., et al., *A Diffusion Model for the Impregnation of Lignocellulosic Materials.* TAPPI Journal, 1997. **80**(11): p. 209-219.

109. Gustafson, R.R., et al., *The Role of Penetration and Diffusion in Nonuniform Pulping of Softwood Chips.* Tappi Journal, 1989. **72**(8): p. 163-167.

110. Tiainen, E., et al., *Determination of Phenolic Hydroxyl Groups in Lignin by Combined Use of ^{1}H NMR and UV Spectroscopy.* Holzforschung, 1999. **53**: p. 529-533.

111. Janes, R.L., *The Chemistry of Wood and Fibers*, in *The Pulping of Wood*, R.G. Macdonald, Editor. 1969, McGraw-Hill. p. 33-72.

112. Smook, G.A., *Handbook for Pulp and Paper Technologists*. 2nd ed. 1992: Angus Wilde Publications.

113. Svedman, M. and P. Tikka, *The Use of Green Liquor and its Derivatives in Improving Kraft Pulping.* TAPPI Journal, 1998. **81**(10): p. 151 – 158.

114. Ban, W. and L.A. Lucia, *Relationship between the kraft green liquor sulfide chemical form and the physical and chemical behavior of softwood chips during pretreatment.* Industrial & Engineering Chemistry Research, 2003. **42**: p. 3831-3837.

115. Fergus, B.J., B.C. Hannah, and R.N. Jones, *The Kraft Pulping and Bleaching of Pinus Radiata Sawdust and Chipper Fines.* Appita, 1973. **27**(2): p. 119-122.

116. MacLeod, J.M. and K.A. Kingsland, *Kraft-AQ pulping of sawdust.* Tappi Journal, 1990. **73**(1): p. 191-3.